การพัฒนาขั้วอิเล็กโทรดของเซลล์เชื้อเพลิงชนิดออกไซด์แข็งแบบ แลนทานัม สตรอนเชียม แมงกาไนต์
ด้วยกระบวนการเมคาโนเคมิคัลขั้นสูง

นายจินตวัฒน์ ไชยชนะวงศ์

DEVELOPMENT OF LANTHANUM STRONTIUM MANGANITE BASED
SOLID OXIDE FUEL CELL ELECTRODE BY ADVANCED
MECHANOCHEMICAL PROCESS

Mr. Jintawat Chaichanawong

A Dissertation Submitted in Partial Fulfillment of the Requirements
for the Degree of Doctor of Engineering Program in Chemical Engineering
Department of Chemical Engineering
Faculty of Engineering
Chulalongkorn University
Academic year 2006

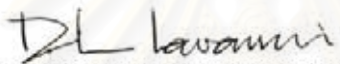|	
Thesis Title	DEVELOPMENT OF LANTHANUM STRONTIUM MANGANITE BASED SOLID OXIDE FUEL CELL ELECTRODE BY ADVANCED MECHANOCHEMICAL PROCESS
By	Mr. Jintawat Chaichanawong
Filed of study	Chemical Engineering
Thesis Advisor	Associate Professor Tawatchai Charinpanitkul, D.Eng.
Thesis Co-advisor	Professor Wiwut Tanthapanichakoon, Ph.D.
Thesis Co-advisor	Professor Makio Naito, D.Eng

Accepted by the Faculty of Engineering, Chulalongkorn University in Partial Fulfillment of the Requirements for the Doctor's Degree
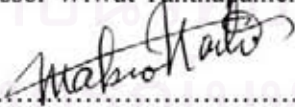
………………………………….. Dean of the Faculty of Engineering

(Professor Direk Lavansiri, Ph.D.)

THESIS COMMITTEE

………………………………….. Chairman

(Associate Professor Suttichai Assabumrungrat, Ph.D.)

…………………………………… Thesis Advisor

(Associate Professor Tawatchai Charinpanitkul, D.Eng.)

………………………………….. Thesis Co-advisor

(Professor Wiwut Tanthapanichakoon, Ph.D.)

………………………………….. Thesis Co-advisor

(Professor Makio Naito, D.Eng)

…………………………………… Member

(Assistant Professor Varong Pavarajarn, Ph.D.)

…………………………………… Member

(Sirapat Pratontep, Ph.D.)

จินตวัฒน์ ไชยชนะวงศ์ : การพัฒนาขั้วอิเล็กโทรดของเซลล์เชื้อเพลิงชนิดออกไซค์แข็งแบบ แลนทานัม สตรอนเชียม แมงกาไนต์ ด้วยกระบวนการเมคาโนเคมิคัลขั้นสูง (DEVELOPMENT OF LANTHANUM STRONTIUM MANGANITE BASED SOLID OXIDE FUEL CELL ELECTRODE BY ADVANCED MECHANOCHEMICAL PROCESS) อ. ที่ปรึกษา : รศ.ดร. ธวัชชัย ชรินพาณิชกุล, อ. ที่ปรึกษาร่วม: ศ.ดร.วิวัฒน์ ตัณฑะพานิชกุล, ศ.ดร.มาคิโอะ ไนโตะ 91 หน้า. ISBN 974-14-3893-1.

งานวิจัยนี้ทำการศึกษาการสังเคราะห์อนุภาค $La_{0.8}Sr_{0.2}MnO_3$ (LSM) ด้วยกระบวนการเมคาโนเคมิคัลขั้นสูงโดยใช้สารผสมเกรดอุตสาหกรรมของอนุภาค La_2O_3, $SrCO_3$ และ Mn_3O_4 กระบวนการบดนี้ไม่มีการใช้ลูกบดและการกระตุ้นเชิงกลเกิดจากการเสียดสีระหว่างอนุภาคผสม โดยภายใต้บรรยากาศชื้น (ความชื้นสัมพัทธ์ 70% ที่ 25 องศาเซลเซียส) ความเข้มของ XRD พีคของอนุภาคสารตั้งต้นจะลดลง และพื้นที่ผิวเฉพาะของสารผสมจะเพิ่มขึ้นในช่วงต้นของการบด (ไม่เกิน 10 นาที) ในการบดเพิ่มต่อจากนั้นพีคของ LSM จะเริ่มปรากฏ การวิเคราะห์การเปลี่ยนแปลงความร้อน (DTA) ชี้ให้เห็นว่าการกระตุ้นเชิงกลนี้นำมาสู่การแตกตัวของ $SrCO_3$ และการเปลี่ยนแปลงเฟสของ Mn_3O_4 โดย จะได้ LSM เฟสเดียวเมื่อเผาอนุภาคผสมที่ถูกบด (เวลาบด 60 นาที) ที่อุณหภูมิต่ำเพียง 900 องศาเซลเซียส ขนาดอนุภาคที่ได้มีขนาดประมาณ 100 นาโนเมตร โดยกระบวนการนี้มีผลให้พบการเจือปนเนื่องจากการปนเปื้อนจากตัวกลางการบดน้อยกว่าวิธีการอื่น นอกจากนี้ได้ศึกษาผลกระทบของปริมาณน้ำตั้งต้นของอนุภาคผสมตั้งต้นต่อการสังเคราะห์ $La_{0.8}Sr_{0.2}MnO_3$ (LSM) ด้วยวิธีเมคาโนเคมิคัล โดยปริมาณน้ำของอนุภาคผสมตั้งต้นถูกปรับให้สูงถึงร้อยละ 2.0 โดยน้ำหนัก ที่ปริมาณน้ำร้อยละ 2.0 โดยน้ำหนัก การเปลี่ยนรูปของผลึกสารตั้งต้นเกิดขึ้นอย่างรวดเร็ว แต่ไม่ทำให้ได้อนุภาคLSM เฟสเดียว ในทางตรงข้ามเมื่อปริมาณน้ำเหมาะสม (น้อยกว่าร้อยละ 0.2 และที่ร้อยละ 0.8 โดยน้ำหนัก) การบดละเอียดเกิดขึ้นในช่วงต้นของการบดและได้อนุภาค LSM เฟสเดียวหลังจากใช้เวลาบด 120 นาที พื้นที่ผิวเฉพาะของอนุภาค LSM เท่ากับ 5.0 ตารางเมตรต่อกรัม และขนาดอนุภาคคำนวณจากพื้นที่ผิวเฉพาะมีค่าประมาณ 180 นาโนเมตร

นอกจากนี้ได้เตรียมอนุภาคคอมพอสิต $La_{0.8}Sr_{0.2}MnO_3$ (LSM)/Y_2O_3 stabilized ZrO_2 (YSZ) ด้วยวิธีเชิงกล โดยการเปลี่ยนสภาวะเชิงกลทำให้ได้อนุภาคคอมพอสิตที่มีการกระจายขนาดอนุภาคแตกต่างกัน 3 ขนาด อนุภาคเหล่านี้ถูกขึ้นรูปเป็นคาโทดของเซลล์เชื้อเพลิงชนิดออกไซค์แข็ง โครงสร้างจุลภาคของคาโทดถูกวิเคราะห์ด้วยกล้องจุลทรรศน์อิเล็กตรอนแบบส่องกราด ความสูญเสียเนื่องจากความต้านทานภายในและโพลาไรเซชันระหว่างอิเล็กโทรไลต์กับคาโทดถูกวัดด้วยเทคนิคเคอเรนท์อินเตอร์รัปชัน คาโทดที่ขึ้นรูปจากอนุภาคคอมพอสิตที่มีการกระจายขนาดอนุภาคแคบจะมีเกรนละเอียด โครงสร้างรูพรุนสม่ำเสมอและมีผิวสัมผัสที่ดีกับชั้นของอิเล็กโทรไลต์ และความสูญเสียเนื่องจากความต้านทานภายในและโพลาไรเซชันจะมีค่าต่ำ ในทางตรงข้ามที่คาโทดที่ขึ้นรูปจากอนุภาคคอมพอสิตที่ประกอบด้วยอนุภาคหยาบจำนวนมาก จะมีเกรนและโครงสร้างรูพรุนที่ไม่สม่ำเสมอ ส่งผลให้ความสูญเสียเนื่องจากความต้านทานภายในและโพลาไรเซชันมีค่าสูง

ภาควิชา.........วิศวกรรมเคมี.............ลายมือชื่อนิสิต.....................................

สาขาวิชา.........วิศวกรรมเคมี.............ลายมือชื่ออาจารย์ที่ปรึกษา.....................

ปีการศึกษา.......2549......................ลายมือชื่ออาจารย์ที่ปรึกษาร่วม...............

ลายมือชื่ออาจารย์ที่ปรึกษาร่วม...............

4671807521   : MAJOR   CHEMICAL ENGINEERING

KEY WORD: $La_{0.8}Sr_{0.2}MnO_3$ / MECHANICAL ACTIVATION / WATER CONTENT / SOFC / PARTICLE SIZE DISTRIBUTION

JINTAWAT CHAICHANAWONG : DEVELOPMENT OF LANTHANUM STRONTIUM MANGANITE BASED SOLID OXIDE FUEL CELL ELECTRODE BY ADVANCED MECHANOCHEMICAL PROCESS. THESIS ADVISOR : ASSOC. PROF. TAWATCHAI CHARINPANITKUL, D.Eng., THESIS CO-ADVISOR : PROF. WIWUT TANTHAPANICHAKOON, Ph.D., PROF. MAKIO NAITO, D. Eng., 91 pp. ISBN 974-14-3893-1.

In this research, synthesis of $La_{0.8}Sr_{0.2}MnO_3$ (LSM) powder by advanced mechanochemical process using a mixture of industrial-grade La_2O_3, $SrCO_3$ and Mn_3O_4 powders was investigated. In the present milling process, no media balls were employed, and mechanical activation was applied through frictions among particles in the powder mixture. Under humid atmosphere (RH 70% at 25 °C), XRD peak intensities of the starting powder decreased, and the specific surface area of the powder mixture increased during the early stage of the milling (<10min). During further milling, the peaks of LSM started to appear. Differential thermal analysis (DTA) suggests that the present mechanical activation brought about the decomposition of $SrCO_3$ and the phase change of Mn_3O_4. Single phase of LSM was obtained by annealing the milled powder mixture (after 60 min of milling) at relatively lower temperature of 900 °C, and its particle size was about 100 nm. The present process resulted in considerably lower release of contamination from the milling media. In addition, the influence of the water content of the starting powder mixture on the mechanochemical synthesis of $La_{0.8}Sr_{0.2}MnO_3$ (LSM) powder was investigated. The water content of the starting powder mixture was varied up to 2.0 wt.%. With water content of 2.0 wt.%, disordering of the crystalline starting powders rapidly proceeded. However, single phase LSM powder was not obtained. At a proper water content (< 0.2 and at 0.8 wt.%), fine grinding of the mixture occurred during the early stage of the milling and single phase LSM powder was obtained after 120 min of milling. The specific surface area (SSA) of the LSM powder was 5.0 m^2/g and the particle size calculated from the SSA was approximately 180 nm.

Furthermore, $La_{0.8}Sr_{0.2}MnO_3$ (LSM)/Y_2O_3 stabilized ZrO_2 (YSZ) composite powders were mechanically prepared. By changing the mechanical conditions, three composite powders with different size distributions were obtained. They were used to fabricate the cathodes of solid oxide fuel cells (SOFCs). Microstructures of the cathodes were carefully characterized by scanning electron microscope (SEM). Losses of internal resistance (IR) and polarization between the electrolyte and the cathode were measured with a current interruption technique. The cathode fabricated from the composite particles with narrow particle size distribution showed fine grains, uniform porous structure, and good contact within the electrolyte layer, and therefore it showed low IR and polarization losses. In contrast, the cathode fabricated from composite particles with large amount of coarse particles exhibited a non-uniform structure in grains and pore structure, resulting in high IR and polarization losses.

Department.......Chemical Engineering...Student's signature. _Jintawat Chaichanawong_

Field of study.....Chemical Engineering...Advisor's signature.....

Academic year...2006.............................Co-advisor's signature.....

Co-advisor's signature.....

ACKNOWLEDGEMENTS

CONTENTS

LIST OF TABLES

LIST OF FIGURES

ABBREVIATIONS

DTA = Differential thermal analysis

D_{50} = Average diameter (50 percentile)

ICP-AES = Inductively coupled plasma atomic emission spectroscopy

IR = Internal resistance

LSM = Lanthanum strontium manganite

LM = Lanthanum manganite

LSM/YSZ = Lanthanum strontium manganite-Ytterium stabilized zirconate

PSD = Particle size distribuition

RH = Relative humidity

SEM = Scanning electron microscopy

SOFC = Solid oxide fuel cell

SSA = Specific surface area (m^2/g)

TPB = Triple phase boundaries

XRD = X-ray Diffraction

YSZ = Ytterium stabilized zirconate

CHAPTER I

INTRODUCTION

1.1   Background

Lanthanum strontium manganite (LSM) is an attractive material because of its high potential for a wide range of applications such as colossal magneto-resistance (Pang et al., 2003; Grossin and Noudem, 2004) and catalytic activities (Hibino et al., 1996). In addition, LSM is a strong candidate for making the cathode electrode of the solid oxide fuel cell (SOFC) because of its good electrochemical properties as well as chemical and thermal compatibilities with the other SOFC components (Minh, 1993; Fukui et al., 2001). It is well known that the SOFC performance is enhanced by improving the electrochemical and electrical properties of the electrodes, which strongly depend on their morphology. The desirable morphology of the SOFC cathode is uniform porous structure, fine grains and good connections of these grains. Therefore, fine LSM powder is necessary for controlling the favorable morphology of the cathode.

Generally, LSM is synthesized either by solid state method (Bell, Millar and Drennan, 2003; Grossin and Noudem, 2004) or chemical solution methods (Bell, et al., 2003; Choi et al., 2004; Ghosh et al., 2005; Gaudon et al., 2002). The solid state method involving a high temperature treatment leads to large particle sizes and limited degree of chemical homogeneity (Cairns et al., 2005). Although the chemical solution methods can produce fine particles, severe control of the processing

conditions is indispensable. Mechanochemical method has also been investigated for the synthesis of various fine particles (Zhang and Saito, 2000; Zhang, Nakagawa and Saito, 2000). Zhang et al. (2000) have mechanochemically synthesized LSM (Composition: $La_{0.7}Sr_{0.3}MnO_3$) from the powder mixture of La_2O_3, SrO, MnO and Mn_2O_3 by a planetary ball milling. Single phase LSM with a specific surface area of about 9 m^2/g was obtained after 180 min of milling.

Recently, Sato et al. (2006) have demonstrated that $LaMnO_{3+\delta}$ (LM) can be mechanochemically synthesized in only 30 min from industrial-grades La_2O_3 and Mn_3O_4 powders. An attrition type milling apparatus was used without any media balls, and a special feature was that milling was to be conducted under humid atmosphere. It was found that the fine grinding enough to trigger the mechanochemical synthesis of LM was achieved at early stage of the milling (10 min), which was mainly due to the formation of $La(OH)_3$ on the surface of La_2O_3 powder. The rapid synthesis without any media balls resulted in considerably lower release of contamination from the milling media.

In this study, the synthesis of LSM by the advanced mechanochemical process without any media balls will be investigated. Industrial-grade La_2O_3, $SrCO_3$ and Mn_3O_4 powders will be used as starting materials. The changes in the crystalline phase, specific surface area, and thermal behavior of the powder mixtures will be shown, and the influence of the mechanical milling on the solid state reaction will be discussed. In addition, the influence of the water content of starting powder mixture on the synthesis of LSM powder will also be investigated.

By the way, solid oxide fuel cells (SOFCs) offer a green technology to generate electricity directly from chemical reactions with high efficiency. Over the last two

decades, SOFCs based on Y_2O_3 stabilized ZrO_2 (YSZ) have been developed for operation in a temperature range of 900-1000ºC (Jørgensen et al., 2001; Jiang and Wang, 2005). More specifically, YSZ was used as the electrolyte, Ni-YSZ cermet as the anode, and $La_{0.8}Sr_{0.2}MnO_3$ (LSM) as the cathode.

Current efforts are aimed at decreasing the operating costs of SOFC by lowering the operating temperatures to 800 ºC or less. To achieve this purpose, the ohmic loss from the electrolyte should be minimized, while the polarization losses at both electrodes should further be decreased (Choi et al., 2000; Leng et al., 2003; Fukui, 1997). To date, the change in cell design and the improvement of powder processing have resulted in significant decreases of these losses for lab-scale planar SOFCs. The polarization losses at both electrodes can be decreased by increasing their electrochemical activity (Minh, 1993). Since electrochemical reaction takes place at triple phase boundaries (TPB) where gaseous species, ions and electrons must be coincident, a microstructure with large TPB leads to a decrease in the polarization loss. Therefore microstructural control of the anode or cathode electrode has kindled interest in this investigation.

Recently, Fukui et al. (2004) have demonstrated that Ni/YSZ composites made from NiO-YSZ composite particles can provide large TPB, and thereby substantially decrease the polarization loss of the anode electrode. As for the cathode, the LSM/YSZ composites have been attempted as well (Fukui et al., 2001). As widely accepted, not only the processing conditions but also the powder characteristics such as particle size distributions (PSD) are important factors to obtain well-controlled microstructures. However, elucidation of PSD influence on the performance of SOFCs has been rather limited.

Therefore, in this study, control of the microstructure of the LSM/YSZ cathode was also attempted by varying the compounding method to obtain LSM/YSZ composite particles. More specifically, the effect of the particle size distribution and microstructure of LSM/YSZ composites on the internal resistance and polarization losses of the cathode will also be investigated.

1.2 Objectives of Study

1. To develop LSM particles for high-performance SOFC electrode by using advanced mechanochemical process.

2. To investigate the influence of particle size distributions of LSM/YSZ composite powders on the microstructure and performance of the SOFC cathode

1.3 Scopes of Study

1. Synthesis of lanthanum strontium manganite by advanced mechanochemical process.

   1.1 The starting materials are La_2O_3, Mn_3O_4 and $SrCO_3$ powders.

   1.2 The average particle sizes of La_2O_3, Mn_3O_4 and $SrCO_3$ powders are about 800, 70 and 400 nm, respectively.

   1.3 The maximum processing time is 120 min.

   1.4 Water content of the starting powder is <0.2-2.0 wt.%.

   1.5 Calcination temperature is $700 - 900 \, ^{o}C$.

2. Study of the influence of particle size distribution of LSM/YSZ composite powder on the microstructure and performance of the SOFC cathode.

2.1 LSM/YSZ composite particles are prepared by advanced mechanochemical process.

2.2 The mixing ratio of LSM:YSZ is 70:30 by weight.

2.3 The maximum processing time is 30 min.

3. Characterize the obtained particles by using SEM (Scanning Electron Microscopy), XRD (X-ray diffraction), BET and TG-DTA (Thermal gravity-Differentiate Temperature analysis). The Fe impurity in the milled and un-milled powders is to be examined by inductively coupled plasma atomic emission spectroscopy (ICP-AES).

1.4   Expected Benefits

1. Single phase LSM with fine particles will be obtained by using advanced mechanochemical process.

2. Comprehension of the influence of the water content of the starting powder mixture on the mechanical synthesis of LSM.

3. Comprehension of the influence of particle size distribution of LSM/YSZ composite powders on the microstructure and performance of SOFC cathode.

CHAPTER II

LITERATURE REVIEW

2.1   Synthesis of Lanthanum Strontium Manganite (LSM)

Bell et al. (2000) synthesized lanthanum strontium manganite (LSM) powder by six different processes, namely solid state reaction, drip pyrolysis, citrate, sol-gel, carbonate and oxalate co-precipitation. It was found that the six samples had similar compositions and surface areas; however, they performed quite differently during catalytic characterization. The surface structure produced by a co-precipitation synthesis route, particularly carbonate, was the most suited to oxidation catalysis, and hence SOFC applications, when compared with other synthesis routes. Drip pyrolysis proved to produce LSM with a high concentration of its surface reaction site, but had poor surface area. The citrate and sol-gel routes produced structures that were by far the least suited in terms of their catalytic activity.

Zhang, Nakagawa and Saito (2000) synthesized perovskite-type strontium manganite ($SrMnO_3$) and LSM powder by grinding the constituent oxides of SrO-MnO_2 and La_2O_3-SrO-Mn_2O_3-MnO_2, respectively, using a planetary mill in air. The synthesis reaction proceeded with an increase in milling time. The product powder of LSM had the morphology of a strong agglomeration of fine grain in nanosize.

Pang et al. (2003) synthesized LSM nanoparticles by a sonication-assisted co-

precipitation method. The advantages obtained by involving ultrasound radiation in the co-precipitation reaction were the lowering of the sintering temperature and a more homogeneous distribution of Mn^{3+} and Mn^{4+} in the structure of LSM nanoparticles. Fully crystalline LSM with an average particle size 24 nm was obtained after the as-prepared mixture was annealed at 900 ^{o}C for 2 h. Mori, Sammes and Tompsett (2000) synthesized LSM by co-precipitation method. Single phase LSM was obtained after heating at 1100 ^{o}C for 1 h. Ghosh et al. (2005) also synthesized lanthanum strontium manganite (LSM) powder by co-precipitation method. It was possible to attain 30-40% open porosity in the sintered LSM with addition of suitable amount of pore former.

Prabhakaran et al. (2005) synthesized nanocrystalline LSM powder in order to use sucrose as a polymerizable fuel. Nitrate salt of La^{3+} and Sr^{2+} and acetate of Mn^{2+} were dissolved in water along with sucrose and concentrated by heating in to the form of a viscous resin which is then transformed into macro porous foam by drying at 120 ^{o}C. Single phase LSM was obtained by combustion of these foams. The LSM powders obtained by planetary milling of the combustion ash possessed particle size in the range 0.1-0.6 μm with a D_{50} value about 0.2 μm. The crystallite size calculated from XRD data using Scherer equation is in the range 13.12 - 17.9 nm.

Kumar et al. (2005) successfully synthesis LSM powder by a novel auto-ignition-induced spray-pyrolysis technique by using a polymerized precursor solution containing citric acid and metal nitrates. The as-sprayed particles appeared to be highly agglomerated with a broad size distribution. Calcination at 750 ^{o}C improved

the particle size distribution. The particles were mainly composed of well-dispersed nanocrystallites of 30-70 nm size.

2.2 Mechanochemical Technique

Zhang and Saito (2000) reported that Perovskite-type lanthanum manganite ($LaMnO_3$) was synthesized by room-temperature milling of La_2O_3 and MnO_3 powders using a planetary ball mill. The synthesis reaction proceeded with the increase in milling time and was finished by about 180 min. The product powder ($LaMnO_3$) was a form of aggregates consisting of fine grains with nanometer grain size. The milled sample had large specific surface area of about 10 m^2/g.

Lee, Zhang and Saito (2001) reported that LaOF could be synthesized through a solid-state reaction between La_2O_3 and LaF_3 by grinding in air. The reaction proceeded with increasing grinding time and was achieved within 60 min. The crystallite size of LaOF in the ground mixture was about 15-20 nm, irrespective of grinding time. Similar reactions occurred in the mixtures of other rare-earth oxide and fluoride systems.

Zhang, Lu and Saito (2002) also reported that $LaCrO_3$ powder could be synthesized mechanochemically by room-temperature grinding of La_2O_3 and hydrous amorphous chromium oxide powder. The obtained $LaCrO_3$ powder sample consisted of agglomerates and large particles due to the water existing in the starting hydrous oxide. This led to relatively low specific surface area of about 5 m^2/g. The

mechanochemical method was also applicable to synthesis of the other rare earth oxides of Pr, Nd or Sm and hydrous chromium oxide.

Ito, Zhang and Saito (2004) synthesized fine lanthanum cobalt oxide (LaCoO$_3$) by two different processes. One was a direct mechanochemical synthesis from oxide. Another process was composed of three steps: grinding a mixture of LaCl$_3$, CoCl$_2$ and NaOH, calcining the ground sample, followed by washing with water to remove NaCl. Both of the methods could synthesize LaCoO$_3$; however, the indirect method was superior to the direct method in terms of the fine LaCoO$_3$ powder due to the dehydration of the hydroxide formed and the high dispersion with NaCl in the ground product. The specific surface area of the final product obtained by indirect process was about 10 m^2/g, which was three times larger than that obtained by the direct process.

Soft mechanochemical synthesis implies a mechanochemical treatment of the starting powders in a liquid media containing hydroxyl groups, i.e. water or various alcohols (Revas Murcury et al., 2004). The influence of water or hydroxyl groups on the mechanical reaction has been extensively investigated and reported by Senna and co-worker (Senna, 1993; Liao and Senna, 1992; 1993; 1995; Watanabe et al., 1996). Senna (1996) reported that rapid complexation was enhanced by the presence of extraordinarily polarized hydroxyl group, due to structure imperfections of the hydroxyl supporting substrates. Mechanochemical reactions of hydroxides or hydrous compounds have also been reported (Fernadez-Rodriguez et al., 1988; Temuujin, Okada and MacKenzie, 1998). Avvakumov et al. (1992; 1994) reported that

mechanochemical reactions in mixtures of hydrated oxide occurred faster than those in anhydrous oxide mixtures.

Liao and Senna (1993) reported that $Mg(OH)_2$ remains crystalline even after intensive vibromilling for 2 days. In grinding it with TiO_2, amorphitation occurred in 2 h, accompanied by dehydration. Baek et al. (1996) also reported that a complex oxide such as $MgTiO_3$ was conventionally prepared by mixing MgO and TiO_2 powders and firing above 1700 K. However, when MgO was replaced with $Mg(OH)_2$, the synthesis becomes much easier. $MgTiO_3$ was observed as a single phase on heating a mechanochemically treated mixture, whereas other mixtures result in different phases.

Garcia-Martinez et al. (2005) reported that galdolinium and dysprosium containing titanate, $Ln_2Ti_2O_7$ and hexagonal Ln_2TiO_5 were successfully prepared at room temperature by milling the constituent oxides in a planetary ball mill using zirconia balls and mortars. Zirconium was observed in the milling product resulting from contamination from the zirconia's container and balls. The amount of Zr measured was typically about 2-4 wt.%.

Shi, Ding and Yin (2000) prepared cobalt ferrite ($CoFe_2O_4$) nanoparticles by the combination of chemical precipitation, mechanochemical method using a planetary ball mill in a hardened steel vial together with several steel balls, and subsequent heat treatment. It was found that Fe contamination in the milling product was about 10 wt.%.

In summary, the mechanochemical method has been investigated for synthesizing ceramic powders including LSM powder. This method enables us to synthesize these ceramic powders at a lower temperature. However, the method required long mechanical milling with media balls, resulting in strong agglomeration.

2.3 Solid Oxide Fuel Cells (SOFCs)

Focusing on the development of SOFC cathode, the suitable materials and fabrication techniques for SOFC cathode are reviewed here. The various techniques to enhance the catalytic activity of the cathode are described. In addition, the relationships of microstructure of SOFC cathode and the system performance are also discussed.

2.3.1 Materials for SOFC cathode

The basic requirements for the cathode material are as follows (Minh, 1993; Singhal, 2000; Steele and Heinzel, 2001; Stambouli and Traversa, 2002; Song, 2002; Webber and Ivers-Tiffée, 2004; Wincewicz and Cooper, 2005):

- High electronic conductivity
- High ionic conductivity
- High porosity
- High catalytic activity
- High stability in an oxidizing environment
- Physical and chemical compatibility with other components (especially electrolyte)
- Low cost

- Easy to fabricate

In conclusion, the SOFC cathode must be electrically conductive, chemically compatible with the electrolyte, and have sufficient porosity to allow gas to be transported to the reaction site. Concerning porosity, an electrode must have enough porosity to allow for gas phase diffusion while maintaining sufficient strength to support the cell during handling and use. In addition, the selection of the cathode material depends on the operating temperature range, cell design, type of electrolyte, and fabrication method.

Among cathode materials reported, lanthanum strontium manganite [(La,Sr)MnO$_3$, (LSM)] is the most extensively studied and investigated materials for SOFC, of which the electrolyte is yttria-stabilized zirconia (Y$_2$O$_3$-ZrO$_2$, YSZ), because LSM has high stability and high electrocatalytic activity for oxygen reduction at high temperature (Jiang, 2003). However, insulating film of lanthanum zirconate (La$_2$Zr$_2$O$_7$) and/or strontium zirconate (SrZrO$_3$) may take place at the interface of an LSM cathode and YSZ electrolyte at temperature above 1200 $^{\circ}$C, thereby decreasing the SOFCs performance (Lee and Oh 1996; Mitsuyasu, Eguchi and Arai, 1997; Brant and Dessemond, 2000; Yang, Wei and Roosen, 2004; Gaudon et al., 2004). Besides, other high ionic conductivity materials have been investigated. Lanthanum strontium ferrite (LSF), lanthanum strontium cobaltite (LSC) (Wincewicz and Cooper, 2005; Inagaki et al., 2000) and lanthanum strontium cobaltite ferrite (LSCF) are the possible candidates to replace LSM at the condition of 600-800 $^{\circ}$C. Unfortunately, direct contact between LSCF and YSZ electrolyte leads to the formation of insulating

SrZrO$_3$ at the LSCF-YSZ interface when sintering the cathode at temperature above 1000 $^{\circ}$C (Stöver, Buchkremer, and Uhlenbruck, 2004).

Yu and Fung (2004) proposed that Sr-doped lanthanum copper oxide (LSCu) with perovskite-based structure was a good candidate cathode material for an IT-SOFC because LSCu/YSZ displays lower cathodic polarization than LSM/YSZ at 800 $^{\circ}$C. In addition, they found that the LSCu exhibited good stability and no phase decomposition was observed after heating the LSCu/YSZ powder mixture at 800 $^{\circ}$C for 1000 h. However, a small amount SrZrO$_3$ was observed when the same mixture was heated at 900 $^{\circ}$C for 10 h. Samarium strontium cobalt was one of the promising cathode materials because it showed higher ionic conductivity than LSM and did not react with galdolinia-doped ceria (GDC) and LSGM electrolyte. However, its cost was still very expensive (Wincewicz and Cooper, 2005; Fukunaga et al., 2000).

2.3.3 Production technique

The production of SOFC cathode can be divided into three steps: powder preparation, cathode fabrication and sintering. However, some productions do not require all the steps shown above. For example, cathode fabrication by flame assisted vapour deposition (FAVD) was able to deposit porous lanthanum strontium manganate (LSM) films for SOFC cathode directly on the electrolyte (Choy et al., 1998; Charojrochkul, Choy, and Steele, 2004; Charojrochkul et al., 2004). In general, after preparation of the starting powder, the cathode is fabricated by screen printing or spraying (for planar design) and extrusion (for tubular design). Then, the fabricated cells were sintered at the designed temperature.

Focusing on the powder processing, the ideal characteristics of the LSM powder for solid oxide fuel cells are that it should be single phase, with a small average particle size and large surface area. In general, LSM powders are synthesized by solid-state reaction method, drip pyrolysis (Bell, Millar and Drennan, 2000), or chemical solution method such as sol-gel (Bell et al., 2000; Choi et al., 2000; Gaudon et al., 2004), citrate route, co-precipitation (Bell et al., 2000; Choi et al., 2000, Jiang and Love, 2003). However, the solid-state reaction method needs high temperature, resulting in large particle size and limited degree of chemical homogeneity. In contrast, the chemical solution methods can produce fine and homogeneous particles with high specific surface area, but the processes are complicated and the reagents used are normally expensive. To solve this problem, mechanochemical method was proposed (Naito, Kondo and Yokoyama, 1993).

Interestingly, nanotechnology is also applicable to SOFC development. For example, LSM composite particles, which consist of both nano-sized LSM and YSZ grains, were successfully prepared by the spray pyrolysis method. The LSM/YSZ composite cathode fabricated by using the composite particles achieved a porous structure as well as uniformly dispersed fine LSM and YSZ grains. Such a unique structure led to high electrochemical activity at 800 ^{o}C (Fukui et al., 1997; Fukui et al., 2001). Furthermore, Gaudon et al. (2004) synthesized the thin film cathode via polymeric method with thickness ranging from 200-1000 nm and with a nanometric grain size distribution. A nanometric grain size distribution when coupled with micro-porosity allows for the presence of a high number of active reaction sites. Film

morphology was modified by changing the intermediate calcination temperatures used in the synthesis of multilayers.

Choi et al. (2000) prepared $La_{0.9}Sr_{0.1}MnO_3$/YSZ cathode from LSM powders of different particle sizes via the silk-printing technique. The mean particle sizes of the three LSM powders were 1.54, 5.98 and 11.31 μm, respectively. The microstructure change was traced by taking scanning electron micrographs at each preparation step. The cathodic activity was monitored by estimating the charge transfer resistance values with the half cell operations. They found that the cathode prepared from 5.98 μm-sized LSM powders gave the best performances in term of initial activity and long term stability because of a large number of its active sites for oxygen reduction and a small number of its active site losses due to particle growth.

Lanthanum strontium cobaltite (LSC) is another interesting cathode material because it possesses ionic and electronic conductivity of a mixed oxide. Inagaki et al. (2000) synthesized LSC by spray pyrolysis. The lowest cathodic polarization is about 25 mV at 300 mA/cm^2. However, the polarization of the LSC cathode increased with operating time because of the interdiffusion of the element at the cathode/electrolyte interface. They suggested that calcinations of the LSC powder could be a potential way to suppress interdiffusion at the interface.

Finally, sintering is another important step because it might directly affect the microstructure of the cathode. Jørgensen et al. (2001) investigated the correlation between the sintering temperature, microstructure and performance of composite

electrodes comprising lanthanum strontium manganate (LSM) and yttria stabilized zirconia (YSZ) with a current collector of LSM at 1000 ^{o}C. The microstructure was found to be less dense and to contain smaller grains as the temperature was decreased in the range of 1300-1500 ^{o}C. This increased the active three-phase-boundary line between electrode, electrolyte and gas phase, leading to a decrease in the polarization resistance with decreasing sintering temperature. In summary, the optimal sintering temperature, at which both the polarization resistance and the series resistance are low, is a trade-off between good physical and electricals contact between LSM and YSZ, and a long TPB.

2.3.4 Recent research and development on SOFC cathode

The main issues of SOFC development are cost reduction by using low-cost materials and simpler processing techniques, and the improvement of performance in long-term operation. In this section, the development of the SOFC cathode was classified into two categories: improvement of material stability and enhancement of catalytic activity.

In the case of high operating temperatures, the development is focused on the stability of cathode materials for long-term operation. Hence, higher stability materials must be chosen as the cathode. However, it is still necessary to improve the material properties due to the economic reason.

In the case of intermediate operating temperatures, the performance of SOFC significantly drops because the conductivity of the cathode dramatically decreases as

the operating temperature decreases below 800 $^{\circ}$C. Therefore, many researchers try to improve the performance of the SOFC. In fact, there are some researches related the development of SOFC for the operating temperatures below 600 $^{\circ}$C (Steele, Hori and Uchino, 2000; Zhu et al., 2003). However, this is not suitable operating condition because of the minimum reforming temperature requirement (Ivers-Tiffée and Weber, 2001) and there is small amount of related information. Therefore, it is not mentioned in this review.

1) Improvement of the materials stability

Two typical ways to improve the stability of cathode materials are to improve the chemical composition of the materials and to control the microstructure. Weber and Ivers-Tiffée (2004) suggested that the interfaces between both electrodes and the thin film electrolyte had to be optimized for low polarization losses and high long-term stability independent of the chemical composition of the electrode materials. Also, Jiang et al. (2003) reported that in the case of LSM cathode, the material microstructure and interface properties were not static but were constantly changing and evolving under polarization or fuel-cell operating condition.

As mentioned previously, it has been reported that LSM can react with YSZ to form an insulating film of lanthanum zirconate ($La_2Zr_2O_7$) and/or strontium zirconate ($SrZrO_3$) near the interface of the LSM cathode and YSZ electrolyte at temperatures above 1200 $^{\circ}$C, thereby decreasing the SOFCs performance (Lee and Oh 1996; Mitsuyasu, Eguchi and Arai, 1997; Brant and Dessemond, 2000; Yang, Wei and Roosen, 2004; Gaudon et al., 2004). Yang et al. (2004) proposed that the formation of

$La_2Zr_2O_7$ and $SrZrO_3$ was due to Mn diffusion to the YSZ. When the content of Mn in the LSM became lower than a threshold value, the LSM became unstable, resulting in the occurrence of excessive La and Sr, and leading to the reaction of Zr with La and Sr. Moreover, Yang et al. (2003) reported that the formation of $La_2Zr_2O_7$ and $SrZrO_3$ in 20% LSM-YSZ system was found after sintering at 1400 ^{o}C for 24 h. However, when the LSM content was increased from 20 to 50 vol.%, more Mn ions were available, and the LSM phase was stable. In short, the reaction between LSM and YSZ occurred less although the diffusion of Mn to YSZ still took place. Therefore, $La_2Zr_2O_7$ and $SrZrO_3$ were seldom found in 50 vol.% LSM-YSZ. Similarly, Jiang et al. (2003) also reported that excess Mn would significantly suppress the formation of $La_2Zr_2O_7$ phase. In short, it is necessary to control the Mn contents in order to limit the insulating phase at the interface of the cathode and electrolyte.

Leng et al. (2005) reported that the LSM/YSZ composite cathode made of A-site deficiency (($La_{0.85}Sr_{0.15})_{0.9}MnO_3$) showed much lower electrode interfacial resistance and overpotential loss (or much better performance) than that made of stoichiometric LSM ($La_{0.85}Sr_{0.15})_{0.9}MnO_3$) because of the formation of $La_2Zr_2O_7$/ $SrZrO_3$ in the composite electrode made of stoichiometric LSM. In addition, A-site non-stoichiometric LSM was more effective in inhibiting $La_2Zr_2O_7$ phase formation than providing excess Mn in the stoichiometric LSM/$MnCO_3$/YSZ electrode.

2.) Enhancement of catalytic activity

Generally, SOFC performance is enhanced by improving the electrochemical, electrical and chemical properties of the electrodes, which depend on their

morphology and chemical composition. It is well known that the performance of SOFCs is mostly influenced by the electrocatalytic activities that depend on the length of the three-phase boundary (TPB), namely, the electrode/electrolyte/pores interface (Minh, 1993; Rambert, McEvoy and Barthel, 1993; Singhal, 2000; Zhao, Virkar, 2000; Jiang 2003; Stambouli and Traversa, 2002; Ghosh, Martel and Tang, 2004). A number of techniques, such as spray pyrolysis (Fukui et al., 1997), vacuum plasma spray (Rambert et al., 1999), sol-gel process (Gaudon et al., 2004; Wu, Liu and Jaegermann, 2005), have been developed to increase the length of the TPB, thereby improving the electrical performance at lower operating temperature. Furthermore, the three phase area would vastly increas when the cathode material had both an intrinsic electronic and ionic conductivity.

Fukunaga et al. (1996) found that the TPB of pure LSM cathode existed only at the interface of YSZ electrolyte, while the TPB of LSM-YSZ composite cathode existed not only on the interface but also in the cathode itself. In addition, the overpotential of the LSM-YSZ composite cathode was lower than that of the pure LSM electrode. It was also found that the overpotential decreased with an increase of the TPB length.

Barbucci et al. (2005) reported that the volume ratio between LSM-YSZ close to 1 gave the best electrochemical activity because of the elongation of the three phase boundary (TPB) in the electrode.

Yang, Wei and Roosen (2003) reported that the conductivity of LSM-YSZ cathode composites was dominated either by YSZ or LSM for the lean or rich contents of LSM phases. For 10 and 20 vol.% LSM-YSZ composite, the hole and oxygen vacancy dominate the conduction below and above the transition temperature of 400 $^{\circ}$C. As the percolation limit was reached (~20 vol.% LSM), the conduction became completely controlled by the LSM phase.

Wang et al. (1998) reported that the best electrochemical performance was obtained with 20 wt.% YSZ addition. Dissociative adsorption of O_2 and the transfer of oxygen ion to the YSZ electrolyte were comparably rate-determining in the oxygen reduction reaction on a pure LSM electrode. With the addition of YSZ, both steps were accelerated due to the enlargement of the TPB area. After YSZ addition, the reaction rate became mainly controlled by the latter step.

In addition, since LSM is a poor ionic conductivity at intermediate temperature (<800 $^{\circ}$C). The use of alternative, higher conductivity electrolytes, such as scandia stabilized zirconia (SYSZ), should enhance the low temperature performance of SOFC. Yamahara et al. (2005) indicated that cobalt post-doping by infiltration of $La_{0.85}Sr_{0.15}MnO_3$-SYSZ composite cathodes had beneficial effects on the performance of anode-supported SYSZ thin-film solid oxide fuel cells between 650-800 $^{\circ}$C. $(La_{0.6}Sr_{0.4})_{1-x}Co_{0.2}Fe_{0.8}O_3/Ce_{0.9}Gd_{0.1}O_3$ (LSCF/CGO) composite cathodes were studied on three types of tape casting electrolyte substrates, including CGO electrolyte, YSZ electrolyte coated with a thin layer of CGO, and YSZ electrolyte (Wang and Mogensen, 2005). High performance of LSCF/CGO composite cathodes has been

obtained in which the polarization resistance (R_p) of 0.19 Ω cm^2 at 600 ^{o}C and 0.026 Ω cm^2 at 700 ^{o}C were achieved on CGO electrolyte. Nano- and submicro-structured cathode is believed to be responsible for such excellent performance.

Moreover, the activation energy of the cathodic reaction may be reduced for the oxygen reaction by adding noble metals such as Au, Ag, Pt, Pd, Ir, Ru or other metals or alloys of the Pt group. However, noble metal catalysts are applied in very tiny amounts to catalyze the electrochemical process at the electrode because of economic reasons. The catalysts are impregnated in the pores of the cathode by chemical process (Ghosh, Martel, and Tang, 2004).

An alternative way to improve the cathode properties is to control the morphology and composition of the cathode starting materials. Nano-particle bonding method, based on mechanochemical method (Naito et al., 1993), is a novel technique to synthesize LSM starting particles without heat treatment by using nanoparticles. The fine grains and long TPB length of the cathode will be achieved; therefore, the performance of SOFC at low operating temperature will be increased.

CHAPTER III

FUNDAMENTAL KNOWLEDGE

3.1 Mechanochemistry

Mechanochemistry deals with an interplay between mechanical energy and chemical state of matter. Mechanochemistry is originally observed from industrial phenomena (i.e., from mineral processing and the related practice of comminution and grinding). Downsizing of solid particles by grinding or milling cannot be made infinitesimally small to individual atoms but is generally limited to a single-micron regime, or at most, to a fraction of micrometer, as far as the size of separately available single particles is concerned. The lower limit of communition comes mainly from two factors: microplasticity and agglomeration. The first concept is understood as an increasing tendency of plastic deformation when the particle size becomes smaller than several micrometers. An increase in the surface free energy promotes agglomeration and prevents powders from limitless size decrease. Fine particles are more than fragments of solids with a smaller dimension. Excess surface energy, which plays an important role in mechanochemistry, is partly due to a small radius of curvature and surface defects. On top of that, downsizing operation brings about severe defects, which are directly combined with surface and bulk chemical properties of solids (Gotoh, Matsuda, and Higashitani, 1997). In mechanochemical phenomena, a portion of the mechanical energy applied is conserved in the solid as different forms of energy to cause a change in its physicochemical properties which eventually gives

an appreciable effect on the chemical reactivity of the solid (Inoya, Gotoh and Higashitani, 1990).

3.2 Solid Oxide Fuel Cells (SOFCs)
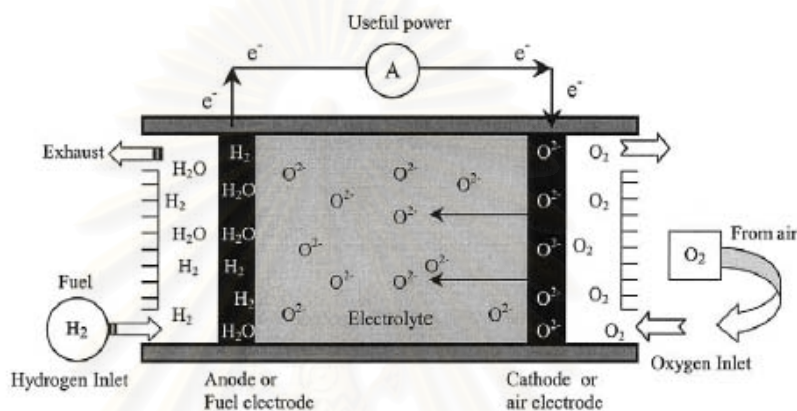
Figure 3.1 Conceptual diagram of solid oxide fuel cell (SOFC)

Solid oxide fuel cell (SOFC) is a solid electrochemical cell which is comprised of a solid oxide electrolyte sandwiched between two electrodes (cathode and anode). The conceptual diagram of the SOFC based on oxygen ion conductors is shown in **Figure 3.1** (Stambouli and Traversa, 2002). Oxygen gas is carried through the cathode to its interface with the electrolyte. Then it is reduced to oxygen ions and move through the electrolyte to the anode. At the anode, the ionic oxygen reacts with fuels such as hydrogen or methane and produce electrons. The electrons travel back to the cathode through an external circuit to generate electric power. SOFCs have several advantages over other types of fuel cells: highest efficiency (50-60%), non-precious materials used, few problems with electrolyte management, fuel adaptability, modularity, possibly internal reforming of hydrocarbon fuel (Jiang, 2003; Minh,

1993; Stambouli and Traversa, 2002). To achieve adequate ionic conductivity in such a ceramic, however, the system must be operated at high temperatures in the range of 650-1000 $^{\circ}$C, typically around 850-1000 $^{\circ}$C in the current technology. The preferred electrolyte material, dense yttria (Y_2O_3)-stabilized zirconia (ZrO_2), is an excellent conductor of negatively charged oxygen (oxide) ion at high temperatures (Song, 2002). The anode of SOFCs is typically a porous nickel-zirconia (Ni-ZrO_2) cermet or cobalt-zirconia (Co-ZrO_2) cermet, while the cathode is typically doped lanthanum manganite especially strontium-doped $LaMnO_3$ (LSM).

CHAPTER IV

PHASE EVOLUTION OF LANTHANUM STRONTIUM

MANGANITE ($La_{0.8}Sr_{0.2}MnO_3$) DURING MILLING BY

ADVANCED MECHANOCHEMICAL PROCESS

4.1 Introduction

Lanthanum strontium manganite (LSM) is an attractive material because of its potential properties for a wide range of applications such as colossal magneto-resistance (Pang et al., 2003; Grossin and Noudem, 2004) and catalytic activities (Hibino et al., 1996). In addition, LSM is a candidate material for cathode electrode for the solid oxide fuel cell (SOFC) because of its good electrical properties and chemical and thermal compatibilities with the other SOFC components (Minh, 1993; Fukui et al., 2001).

Generally, LSM is synthesized by solid state method (Bell, Millar and Drennan, 2003; Grossin and Noudem, 2004) and chemical solution methods (Bell, et al., 2003; Choi et al., 2004; Ghosh et al., 2005; Gaudon et al., 2002). The solid state method involving a high temperature treatment leads to large particle sizes and a limited degree of chemical homogeneity (Cairns et al., 2005). Although the chemical solution methods can produce fine particles, severe control of the processing conditions is strictly required. Mechanochemical methods have also been investigated for the synthesis of various fine particles (Zhang and Saito, 2000; Zhang, Nakagawa and Saito, 2000). Zhang et al. (2000) mechanochemically synthesized LSM (Composition: $La_{0.7}Sr_{0.3}MnO_3$) from the powder mixture of La_2O_3, SrO, MnO and Mn_2O_3 by a

planetary ball milling. The single phase of LSM with the specific surface area of about 9 m^2/g was obtained after 180 min of milling.

Recently, Sato et al. (2006) have demonstrated that $LaMnO_{3+\delta}$ (LM) can be mechanochemically synthesized after milling for only 30 min from industrial grades of La_2O_3 and Mn_3O_4 powders. An attrition type milling apparatus was used without any media balls, and a special feature of the milling was to do it under humid atmosphere. It was found that the fine grinding sufficient to trigger the mechanochemical synthesis of LM was achieved at an early stage of the milling (10 min), which mainly due to the formation of $La(OH)_3$ on the surface of La_2O_3 powder. The rapid synthesis without any media balls resulted in considerably less contamination released from the milling media.

In this study, mechanical milling without any media balls under controlled atmosphere was conducted on industrial grade La_2O_3, $SrCO_3$ and Mn_3O_4 powders, aiming at LSM formation. The powder mixture containing alkaline-earth carbonates is interesting from a practical viewpoint. $SrCO_3$ is quite stable whereas the carbonation of SrO is unavoidable during storage under the ambient condition. Changes in the crystalline phase, specific surface area, and thermal behavior of the powder mixtures are shown, and the influence of the mechanical milling on the solid state reaction will be discussed.

4.2 Experimental

The starting materials were industrial grade La_2O_3 (purity: 99.99%, KCM Corp., Japan), $SrCO_3$ (97% KCM Corp., Japan) and Mn_3O_4 (99% KCM Corp., Japan) powders. Their average particle sizes as calculated from the specific surface area were

about 800, 400 and 70 nm, respectively. They were mixed at the stoichiometric molar

ratio of cations as La: Sr: Mn = 0.8: 0.2: 1. 70 g of the powder mixture was put into a

chamber and mechanically activated using the attrition type milling apparatus

illustrated in **Figure 4.1** (Sato et al., 2006). Its main components were a fixed

chamber and a rotor set with a certain clearance against the internal surface of the

chamber. Both the chamber and the rotor were made from stainless steel. The rotating

speed of the rotor was 3000 rpm and the total milling time was 60 min. Humid air was

admitted into the chamber before the milling started, and the milling was performed

under the humid atmosphere (RH 70%). Generally, the temperature of the chamber

rose significantly because of high frictional losses during milling. Without any

cooling water, the temperature of the chamber could rise above 500 ^{o}C. In this study,

the temperature of the chamber during milling was therefore controlled by cooling

water. Consequently, the average temperature of the chamber was about 120-150 ^{o}C.

After the milling, about 95% of the powder mixture was recovered from the chamber

regardless of atmospheric condition. Finally, the powder mixture was heated in order

to obtain the single-phase LSM. Meanwhile, the un-milled powder mixture was also

heated to compare this mechanical method with the conventional solid state method.

Phase evolution during the milling was examined by XRD measurement (JDX-

3530M, JEOL, Japan) using Ni filtered CuKα radiation as X-ray source. The XRD

patterns were collected in the range of 10-70 ^{o} with a step size of 0.02 ^{o}. The specific

surface areas (SSA) of the starting and the milled powder mixtures were measured

with the nitrogen gas adsorption instrument (Micromeritics ASAP 2010, Shimadzu,

Japan) based on the BET method with sample mass of about 2 g. The powder

mixtures were dried at 200 ^{o}C for 12 h before the SSA measurement. The thermal

behaviors for the starting and the milled powder mixtures were examined by the differential thermal analysis (DTA). The DTA curves were obtained up to 900 ºC under air flow (flow rate: 300 ml/min) with sample mass of about 13 mg at a heating rate of 10 ºC/min.
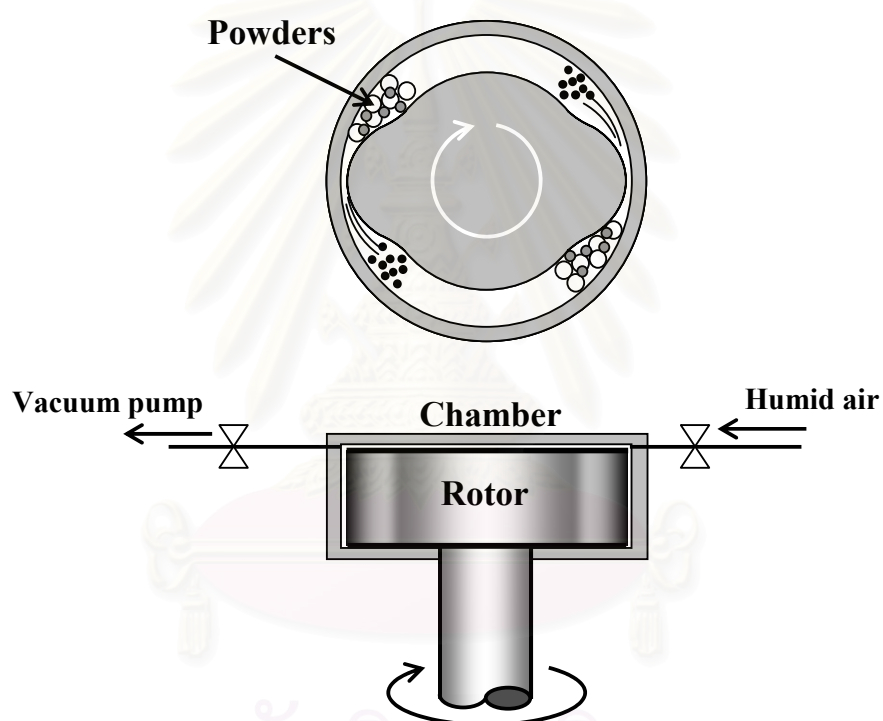
Figure 4.1 Schematic illustration of the milling apparatus

4.3   Results and Discussion

4.3.1   Phase evolution by mechanical activation

Figure 4.2 shows the phase evolution of the powder mixture as a function of the milling time. Peaks of La_2O_3, $SrCO_3$ and Mn_3O_4 were clearly observed before the milling. After milling for 10 min, the peak intensities of the starting powders slightly decreased, and the new peaks identified as $La(OH)_3$ appeared. The formation of $La(OH)_3$ was due to the hydration of La_2O_3 during the milling (Sato et al., 2006). After milling for 20 min, the peak intensities of the starting powders decreased further. In addition, the peaks corresponding to the LSM started to appear. Continued milling reduced the peak intensities of the starting powders. On the other hand, the intensity of LSM remained almost constant. The results suggest that the mechanical energy supplied during milling after the first 10 min was utilized mainly for disordering the crystalline structure of the starting powders.
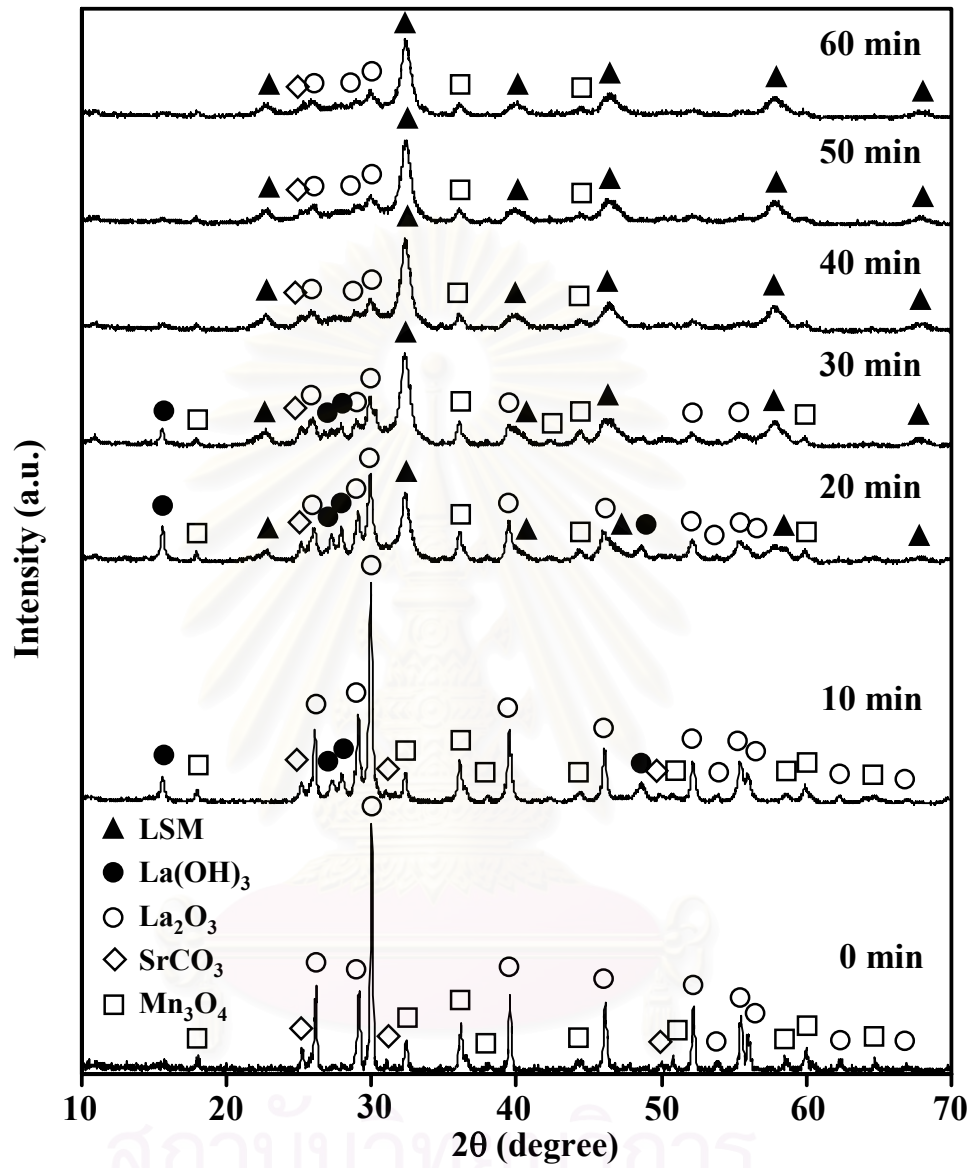
Figure 4.2 XRD patterns of starting and milled powder mixtures

Table 4.1 Specific surface area (SSA) of starting and milled powders.

Milling time (min)	0	10	20	30	40	50	60
SSA (m^2/g)	6.5	8.1	6.5	5.7	4.3	3.7	3.5

Table 4.1 shows the change in the SSA of the powder mixture with the milling time. After 10 min of the milling, the SSA increased from 6.5 to 8.1m^2/g. Then, the SSA gradually decreased as the milling time increased. Similar behavior has been observed and reported on the milling of various powder mixtures (Fu and Wei, 1996; Ito, Zhang and Saito, 2004). In the present case, the fine grinding occurred more preferentially than the agglomeration of the powder mixture during the first 10 min. However, mechanical energy supplied during milling after 10 min could be utilized for agglomeration.

After the SSA reached a maximum (10 min), the peaks corresponding to the LSM appeared and those of the starting powders significantly decreased on the XRD patterns. This shows that the increase of the SSA and the disordering of crystalline structures of the raw substances are of vital importance for solid state reaction of LSM in the present milling. In this case, the formation of La(OH)$_3$ is considered to be a key step. La$_2$O$_3$ is easily hydrated in the presence of water vapor, while Mn$_3$O$_4$ and SrCO$_3$ are not. Generally, the mechanical hardness of metal hydroxides is significantly lower than their corresponding oxides. Therefore, the Mn$_3$O$_4$ and SrCO$_3$ powders would act as media balls and preferentially grind out the La(OH)$_3$ formed on the surface of La$_2$O$_3$ powder, resulting in the increase of the SSA. Consequently, a large area of

contacts between the reactant substances would be achieved. Such a microscopic mixing state would promote the solid state reaction of LSM. However, the mixing state that triggers the solid state reaction should further be investigated with TEM-EDS tools.

To substantiate the effect of the fine grinding of La_2O_3 on the formation of LSM during mechanical milling, finer La_2O_3 powder with average particle size about 200 nm was used as starting powder instead of coarse La_2O_3 powder (800 nm). **Figure 4.3** shows the phase evolution of the powder mixture as a function of the milling time when finer La_2O_3 was used. Peaks of La_2O_3, $SrCO_3$ and Mn_3O_4 were clearly observed before the milling. It is obvious that, after milling for 10 min, the peak intensities of the starting powders suddenly decreased, and the peaks of LSM started to appear. After milling for 20 min, the peak intensities of the starting powders decreased further. The intensity of LSM peak increased as the milling time increased. The SSA of the starting powder mixture, and the powder mixtures after 10 and 20 min of milling were 8.4, 6.8 and 6.2 m^2/g, respectively. The results suggest that after the first 10 min the mechanical energy supplied during milling was utilized mainly for disordering the crystalline structure of the starting powders. In addition, a large area of contacts between the reactant substances would be achieved rapidly because of the high SSA of the starting powder mixture. As mentioned previously, this microscopic mixing state would promote the solid state reaction of LSM, thereby leading to more rapid formation of LSM than using a coarse La_2O_3 powder as starting powder. It is confirmed that the fine grinding of La_2O_3 during the early state of milling is an important step to initiate the formation of LSM.
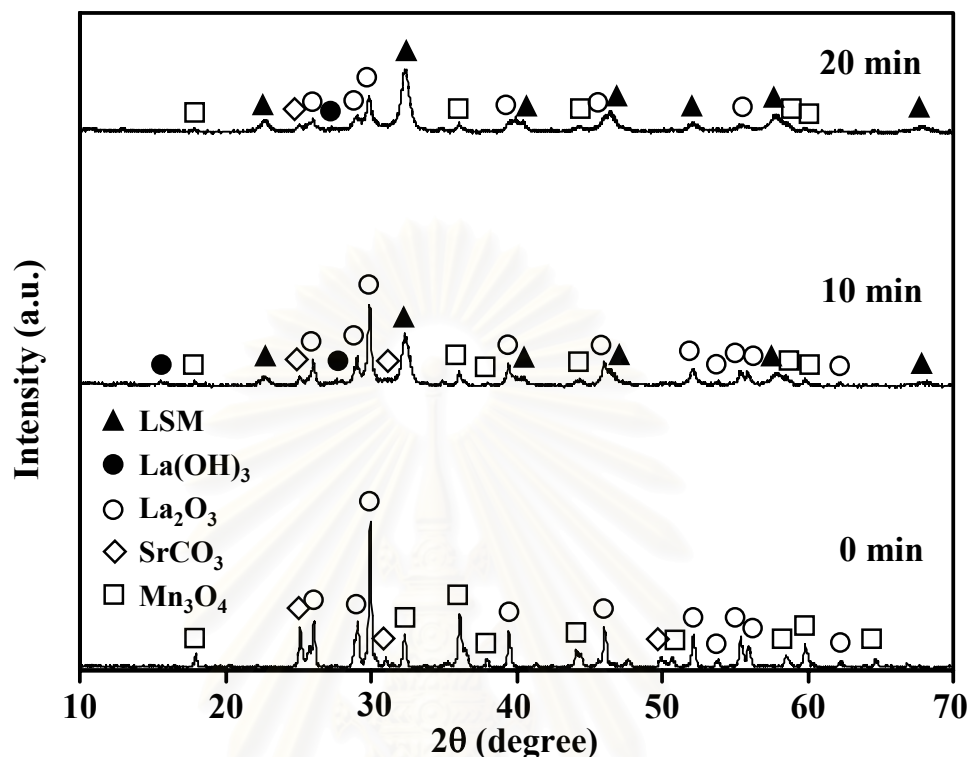
Figure 4.3 XRD patterns of starting and milled powder mixtures when a finer La_2O_3 powder was used as starting powder.

4.3.2 DTA results

Figure 4.4 shows the DTA curves of the starting and the milled powder mixtures. For the starting powder mixture, an exothermic peak was observed at 560 $^\circ$C, which indicates the oxidation of Mn_3O_4 ($2Mn_3O_4 + 1/2O_2 \rightarrow 3Mn_2O_3$) (Fritsch et al., 1998; Gillot, El Guendouzi and Laarj, 2001). Then, an endothermic event was observed at 880 $^\circ$C, which may be ascribed to the decomposition of $SrCO_3$ ($SrCO_3 \rightarrow SrO + CO_2$) (Berbenni, Marini and Bruni, 2001). There was no peak associated with the LSM formation in the whole temperature range.

For the milled powder mixtures, endothermic peak intensities for $SrCO_3$ decomposition decreased with increasing milling time and disappeared after the

milling took place for 60 min. This change is consistent with the XRD patterns, in which the peak intensity of $SrCO_3$ decreased with the increasing milling time.

For the powder mixtures milled over 10 min, the exothermic peak related to the oxidation of Mn_3O_4 became inconspicuous. An experiment was carried out in order to verify the phenomenon. When milling only the Mn_3O_4 powder, the phase change ($2Mn_3O_4 + 1/2O_2 \rightarrow 3Mn_2O_3$) was clearly observed on the XRD patterns. Although the oxidized Mn_3O_4, i.e., Mn_2O_3, was not observed in the XRD patterns of the milled powder mixtures as shown in **Figure 4.2**, the disordering of the Mn_3O_4 powder would be achieved by the present mechanical activation through its phase change. The change in the valence must have occurred with the present mechanical activation through the phase change of Mn_3O_4. In this study, the LSM was formed from the powder mixture involving Mn_3O_4. The average valence of manganese should be +3 in the perovskite LSM lattice (Chen, Khor and Chan, 2004) but it is +2.67 in Mn_3O_4. Therefore, the average valence of manganese increased during the formation of LSM in the present milling. In a previous study, perovskite LM powder was also synthesized when La_2O_3 and Mn_3O_4 was milled in the same manner (Sato et al., 2006). The valence change associated with the mechanochemical synthesis should be investigated further.

Figure 4.5 shows the XRD patterns after heat treatments of the powder mixture milled for 60 min. Only slight increases in the peak intensities for LSM were observed after the heating at 700 $^\circ$C. Drastic increases of the peak intensities were observed above 800 $^\circ$C. Finally, single phase LSM was obtained at 900 ºC. Therefore, the exothermic peaks at around 800 ºC on the DTA for the powder mixtures milled

over 20 min corresponded to the formation of LSM from the unreacted substances in the milled powder mixtures.
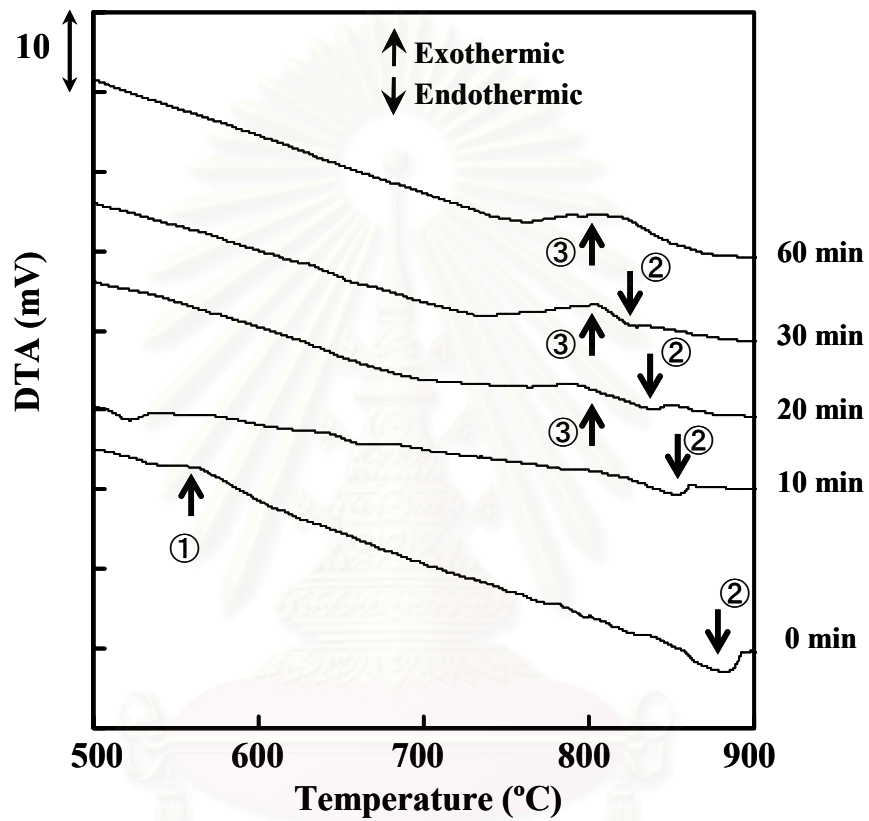
Figure 4.4 DTA curves of starting and milled powder mixtures. Peaks correspond to
① $2Mn_3O_4 + 1/2O_2 \rightarrow 3Mn_2O_3$, ② $SrCO_3 \rightarrow SrO + CO_2$ and ③ LSM formation
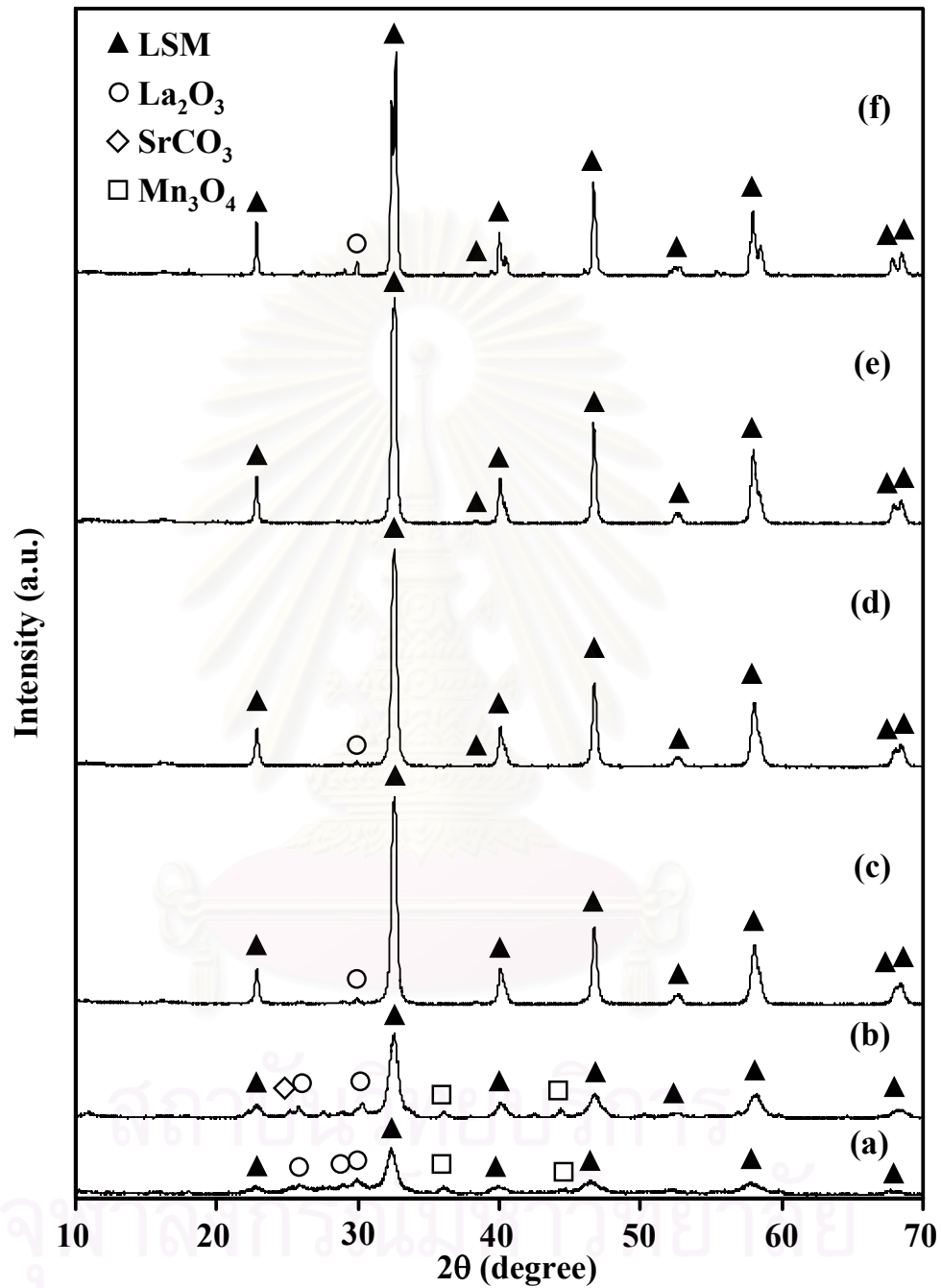
Figure 4.5 XRD patterns of processed powders: (a) milled powder for 60 min; (b) the

powder mixture milled for 60 min, followed by heating at 700 ºC ; (c) 800 ºC; (d) 850

ºC; (e) 900ºC; (f) the un-milled powder heated at 1200 ºC

4.4   Conclusion

In this study, mechanical milling of a powder mixture of industrial-grade La_2O_3, $SrCO_3$ and Mn_3O_4 powders was conducted under a humid atmosphere (RH70% at 25 ℃). An attrition type milling apparatus was used without any media balls, which presented the mechanical activation through friction among particles during the milling. The XRD peak intensities of La_2O_3 $SrCO_3$ and Mn_3O_4 decreased, and the specific surface area of the powder mixture increased at the early stage of the milling (<10min). After milling for 20 min, the lanthanum strontium manganite (LSM) started to appear. Additional milling further reduced peak intensities of the starting powders. However, the intensity of LSM remained almost constant. DTA analysis revealed that the use of the present mechanical activation accelerated the decomposition of $SrCO_3$ and the phase change of Mn_3O_4.

CHAPTER V

LOW TEMPERATURE SYNTHESIS OF LANTHANUM

STRONTIUM MANGANITE (La$_{0.8}$Sr$_{0.2}$MnO$_3$) BY

ADVANCED MECHANOCHEMICAL PROCESS

5.1 Introduction

As mentioned in 4.1, lanthanum strontium manganite (LSM) is an attractive material because of its potential properties for a wide range of applications such as colossal magneto-resistance (Pang et al., 2003; Grossin and Noudem, 2004) and catalytic activities (Hibino et al., 1996). In addition, LSM is a candidate cathode material for the solid oxide fuel cell (SOFC) because of its good electrical conductivity, catalytic activity for reduction of oxygen, and chemical and thermal compatibilities with other SOFC components (Minh, 1993; Fukui et al., 2001). It is well known that the SOFC performance is enhanced by improving the electrochemical and electrical properties of the electrodes, which strongly depend on their morphology. The morphology of the SOFC cathode should be homogeneously porous structure, fine grains and good connection of these grains. Therefore, fine LSM powder is necessary for controlling the favorable morphology of the cathode.

Generally, LSM is synthesized by solid state reaction (Grossin and Noudem, 2004; Bell, Millar and Drennan, 2003) and chemical solution methods (Bell, et al., 2003; Choi et al., 2004; Ghosh et al., 2005; Gaudon et al., 2002). However, the solid state method, involving high temperature synthesis, leads to large particle sizes and a limited degree of chemical homogeneity. In addition, the method often comprises a

multi-step process resulting in high level contamination (Cairns et al., 2005). Although the chemical solution methods can produce chemically homogeneous fine particles, severe control of the processing conditions is required. The production cost of the nano-powder by the solution method is commonly higher than the solid state method. The mechanochemical method has also been investigated for synthesizing ceramic powders including LSM powder (Zhang and Saito, 2000; Zhang, Nakagawa and Saito, 2000). This method enables us to synthesize the ceramic powders at a lower temperature. However, the method required long mechanical milling with media balls, resulting in strong agglomeration (Zhang, Nakagawa and Saito, 2000) and contamination due to the wear of the media balls and the chamber wall during the milling (Shi, Ding and Yin, 2000; Garcia-Martinez et al., 2005; Algueró, Ricote and Castro, 2004).

Recently, Sato et al. (2006) have developed an advanced mechanochemical process without ball media for synthesizing lanthanum manganite. The apparatus used consisted of just a fixed vessel and a rotor set with a certain clearance against the inside wall of the vessel. Both the vessel and the rotor were made from stainless steel. When the rotor was rotating, the powder mixture was compressed into the clearance and received various kinds of mechanical forces such as compression and shearing. The product synthesized through this process showed fine particles product and lower contamination compared to the other mechanical processes. It is therefore expected that this method would be applicable for synthesizing LSM.

In the present research work, the formation of LSM by means of the advanced mechanochemical process would be investigated. The composition of $La_{0.8}Sr_{0.2}MnO_3$ was chosen because the composition was widely used for SOFC application. The

influence of additional heat treatment on the synthesis of LSM from as-milled powders would also be investigated.

5.2 Experimental

The starting powder materials were industrial-grade La_2O_3 (99.99%, KCM Corp., Japan), $SrCO_3$ (99% KCM Corp., Japan) and Mn_3O_4 (99% KCM Corp., Japan) powders. Their average particle sizes as calculated from the specific surface area (SSA) were about 800, 400 and 70 nm, respectively. They were mixed at the molar ratio of cations as La: Sr: Mn = 0.8:0.2:1. Total amount of 70 g of the mixture was milled by the advanced mechanochemical method without media balls illustrated in **Figure 4.1** (Sato et al., 2006) for different periods of time. Its main components were a fixed chamber and a rotor set with a certain clearance against the internal surface of the chamber. Both the chamber and the rotor were made from stainless steel. When the rotor was rotating, the powder mixture was compressed into the clearance (1 mm in gap) and receives various kinds of mechanical forces such as compression and shearing. The rotating speed of the rotor was 3000 rpm. Humid air was admitted into the chamber before the milling started, and the milling was performed under the humid atmosphere (RH 70%). After the milling, the powder mixture was heated in order to obtain the single phase of LSM. Meanwhile, the un-milled powder mixture was also heated to compare this mechanical method with the conventional solid state method. Phase identification was conducted by the X-ray diffraction method (XRD: JDX-3530M, JEOL, Japan) using CuKα radiation as X-ray source for the milled and un-milled powders before and after heat treatment. The XRD patterns were collected in the range of 10-70º with a step size of 0.02º. The specific surface areas (SSA) of

the as-milled and processed powder were measured by a nitrogen gas adsorption instrument (Micromeritics ASAP 2010, Shimadzu, Japan) based on the BET method. The morphology of the LSM powder was observed by scanning electron microscopy (SEM, ERA-8800FE, Elionics, Japan). The Fe impurity in the milled and un-milled powders was examined by inductively coupled plasma atomic emission spectroscopy (ICP-AES: SPS5100, SII NanoTechnology Inc., Japan).

5.3   Results and Discussion

Figure 4.2 shows the XRD patterns of the starting powder mixture and those milled for 10, 20 and 40 min. There were only peaks of La_2O_3, $SrCO_3$ and Mn_3O_4 at the start. After milling for 10 min, the peak intensities of the starting powder slightly decreased, and the peaks of $La(OH)_3$ were observed. This can be ascribed to the hydration of La_2O_3 during milling by the moisture of the charged ambient air. It is noted that the peaks corresponding to LSM started to appear only after 20 min of milling without any heating. This suggests that the mechanical forces applied by milling were utilized efficiently for the formation of LSM during the first 20 min. The peaks of $La(OH)_3$ were not observed after 40 min. The peak intensities of the LSM increased during the period from 20 to 40 min.

Table 4.1 shows the change in the specific surface area (SSA) of the powder mixture with the increase in milling time. The SSA of the starting powder mixture was 6.5 m^2/g. It dramatically increased to 8.1 m^2/g after milling for 10 min, and then it decreased to 6.5 m^2/g at 20 min. The results imply that the mechanical forces applied by milling contributed to the fine grinding of the powder mixture during the first 10 min of milling, resulting in the significant increase in the SSA. The rapid

formation of the LSM can be attributed to the intimate microscopic mixing achieved during the early stage of the milling.

In order to obtain the single phase LSM, the milled powder at 60 min was chosen and calcined at different temperatures. Meanwhile, the un-milled powder mixture was also heated at 1200 ^{o}C for 6 h. **Figure 4.3 (a) - (e)** shows the phase evolutions of the powder mixture milled for 60 min followed by heat treatment at 700, 800, 850, and 900 ^{o}C, respectively. Only a minor peak associated with the unreacted La_2O_3 was observed for powders heated under 850 ℃. Single phase LSM was successfully obtained after heating at 900 ℃ for 6 h. In contrast, single phase LSM could not be obtained from the un-milled powder despite heat treatment at 1200 ℃ (**Figure 4.3 (f)**). The results indicate that the powder was effectively activated by milling, so that it reacted completely at only 900 ℃.

Figure 5.1 shows a SEM micrograph of the LSM powder synthesized by the mechanical milling for 60 min followed by heating at 900 ℃ for 6 h. The size of primary particles observed from the micrograph was about 100 nm. The SSA of the powder was 10.6 m^{2}/g. The average particle size calculated from the SSA was about 90 nm. The obtained small particle size of the LSM can be ascribed to the mechanical activation which involves fine grinding, precise mixing and disordering the crystalline structures of the starting powders during milling, and so can the resultant lower calcination temperature.
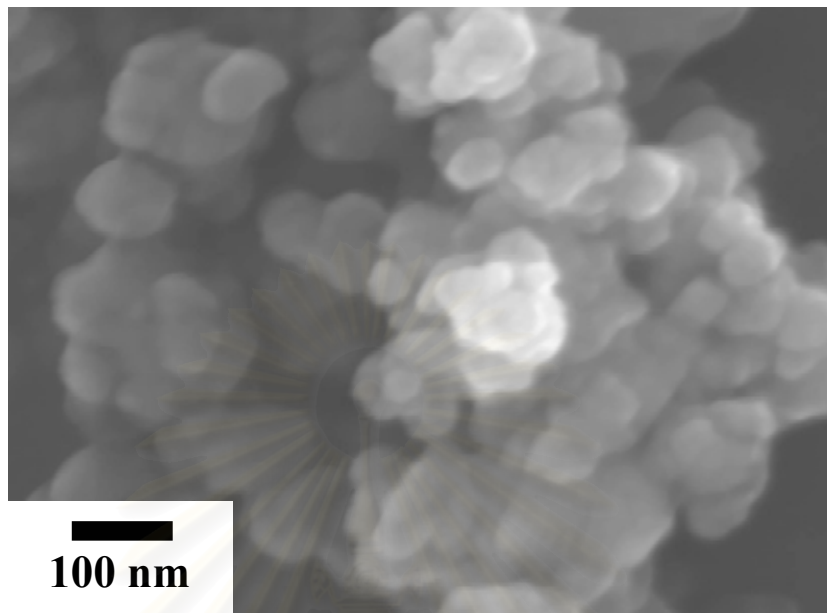
Figure 5.1 SEM micrograph of LSM powder synthesized by milling for 60 min, followed by heating at 900 ℃

Since the material of the construction of the apparatus used was stainless steel, Fe might be released by the wear of the chamber wall and the rotor during the milling. **Table 5.1** shows the amount of Fe impurity in the starting and the milled powder mixtures.

Table 5.1 Amount of Fe impurity in the starting and milled powders

Milling time (min)	0	30	60
Fe impurity (ppm in mass)	34	55	52

The Fe impurities of the starting and the milled powder mixtures were 34 ppm, 55 ppm (30 min milling) and 52 ppm (60 min milling) in mass, respectively. After deducting the Fe impurity in the starting powders, the amount of Fe contamination contributed by the milling was about 20 ppm in mass. The degree of the contamination during the milling was considerably lower than that of the previous studies (Shi, Ding and Yin, 2000; Garcia-Martinez et al., 2005; Algueró, Ricote and Castro, 2004). The low Fe contamination can be attributed to the short period of milling and the absence of ball media. The results suggest that the present approach is one of the most promising methods for synthesizing high quality fine powders with low contamination.

In addition, a preliminary experiment was conducted in order to test the performance of a solid oxide fuel cell (SOFC) which used LSM powder from this process as the cathode. The fabrication and testing of the SOFC was conducted by Sato et al. (in press), the details of which will be published elsewhere. The electrolyte thin film was prepared by tape casting from the slurry of YSZ powder (TZ-8Y, Tosoh Inc., Japan), ethanol and binders. The film was dried under ambient air for 24 h. The NiO (F-Type, Nicoh Rita Corp.,Japan)-YSZ composite powders (mass ratio NiO:YSZ = 65.6:34.4) were milled by advanced mechanical method (Mechanofusion system, Model AM-20F, Hosokawa Micron Corp., Japan). Next, NiO-YSZ film (~750 μm in thickness) was formed on the electrolyte film by tape casting the slurry composed of the NiO-YSZ powder mixture, ethanol and binders. Then, the bilayer film of YSZ/NiO-YSZ was dried and co-sintered in the air at 1350 ^{o}C for 2 h. The LSM powder was prepared by the advanced mechanochemical process and subsequently heated in the air at 900 ^{o}C for 6 h. The LSM powder was mixed with ethylene-glycol,

screen printed on the sintered YSZ/NiO-YSZ bilayer, and then sintered in the air at 1100 ^{o}C for 2 h. Cell performance of the anode supported SOFC was tested at the operating temperature of 800 ^{o}C while supplying 97% H_2 - 3% H_2O to the anode and air to the cathode. The open circuit voltage was found to be 1.1 V at 800 ^{o}C, indicating that the film was dense enough to prevent gas leakage through it. The maximum power density of SOFC was 0.75 W/cm^2. This result is comparable with that of the intermediate temperature SOFC based on an anode supported SOFC prepared by Yamaji et al. (2004) (~0.55 W/m^2, cathode/electrolyte/anode: LSM/ScSZ/NiO-ScSz), Haanappel et al. (2005) (~0.75 W/m^2, multilayer cathode/electrolyte/anode: LSM-YSZ and LSM/YSZ/Ni-YSZ), and Kim et al. (2005) (~0.5 W/m^2, multilayer cathode/electrolyte/anode: LSM-YSZ, LSM and LSCF/YSZ/Ni-YSZ). In addition, Choi et al. (2000) prepared $La_{0.9}Sr_{0.1}MnO_3$/YSZ cathodes from LSM powders of different particle sizes via the silk-printing technique. The mean particle sizes of the three LSM powders were 1.54, 5.98 and 11.31 μm, respectively. The cathodic activity was monitored by estimating the charge transfer resistance values with the half cell operations. The cathode prepared from 5.98 μm-sized LSM powders gave the best performance in term of initial activity and long term stability because of a large number of its active sites for oxygen reduction and a small number of its active site losses due to particle growth. However, the influence of fine LSM particle on the microstructure and the performance of SOFC, and the optimum particle size of LSM powder should be investigated further.

5.4   Conclusion

Formation of lanthanum strontium manganite (LSM) was observed after only 20 min of milling without any heating. The rapid formation of LSM can be attributed to the intimate microscopic mixing achieved during the early stage of the milling. The influence of heat assistance on the synthesis of LSM was also investigated. Single phase LSM was obtained by heating and holding the powder mixture milled for 60 min at 900 $^\circ$C for 6 hours. The lower synthesis temperature, when compared to the conventional solid state process, is attributed to the mechanical activation of the advanced mechanochemical process. A short milling time of 60 min and a low synthesis temperature of 900 $^\circ$C resulted in fine LSM particles with the average particle size of 90 nm. Furthermore, the advanced mechanochemical process without ball media and with short milling time brings the advantage of lower Fe contamination compared with the other mechanical methods.

CHAPTER VI

INFLUENCE OF THE WATER CONTENT OF THE STARTING POWDER MIXTURE ON THE MECHANOCHEMICAL SYNTHESIS OF LANTHANUM STRONTIUM MANGANITE

6.1 Introduction

As mentioned in section 4.1, mechanochemical methods have been investigated for the synthesis of various fine particles including LSM powder (Zhang and Saito, 2000; Zhang, Nakagawa and Saito, 2000). Recently, Sato et al. (2006) have demonstrated that $LaMnO_{3+\delta}$ (LM) can be mechanochemically synthesized after milling for only 30 min from industrial-grade La_2O_3 and Mn_3O_4 powders. An attrition type milling apparatus was used without any media balls, and a special feature of the milling was to do it under humid atmosphere. It was found that the fine grinding sufficient to trigger the mechanochemical synthesis of LM was achieved at an early stage of the milling (10 min), mainly due to the formation of $La(OH)_3$ on the surface of La_2O_3 powder.

The influence of water or hydroxyl groups on mechanically induced reaction (soft mechanochemical reactions) has extensively been investigated and reported by Senna and co-workers (Senna, 1993; 1996; Liao and Senna, 1992; 1993; 1995; Watanabe et al., 1996). Senna (1996) reported that rapid complexation was enhanced by the presence of extraordinarily polarized hydroxyl groups due to structural

imperfections of the hydroxyl supporting substrates. Mechanochemical reactions of hydroxides or hydrous compounds have also been reported (Fernadez-Rodriguez et al., 1988; Temuujin, Okada and MacKenzie, 1998). Avvakumov et al. (1992; 1994) reported that mechanochemical reactions in mixtures of hydrated oxide occurred faster than those in anhydrous oxide mixtures. However, it has been reported that after mechanochemical reaction, the water in Cr_2O_3-nH_2O has been transferred as free water, which works like a binder combining fine particles in agglomerates into one large particle (Zhang et al., 2002). The proper water content in a starting powder for the synthesis of fine particles without reducing the reactivity is under investigation.

In this study, mechanical milling without any media balls was conducted on industrial-grade La_2O_3, $SrCO_3$ and Mn_3O_4 powders by varying the water content of these starting powder mixtures. Phase evolution and specific surface area of the milled powders are shown, and the influence of the water content of the starting powder mixture on the formation of LSM will be discussed. The proper water content of starting powder mixtures for the synthesis of LSM powder will also be reported.

6.2 Experimental

The starting materials were industrial-grade La_2O_3 (purity: 99.99%, KCM Corp., Japan), $SrCO_3$ (97%, KCM Corp., Japan) and Mn_3O_4 (99%, KCM Corp., Japan) powders. Their average particle sizes as calculated from the specific surface area were about 800, 400 and 70 nm, respectively. They were mixed at the stoichiometric molar ratio of the cations as La: Sr: Mn = 0.8: 0.2: 1. The water content in the starting powder mixture was varied from the dry state up to 2.0 wt. % by exposing the dry starting powders to humid atmosphere (RH 80%, 25 ^{o}C). The weight of the powder

mixture was measured before and after exposure to the humid atmosphere in order to calculate the water content of the starting powder mixture. Then, the powder mixture was put into a chamber and mechanically activated using the attrition type milling apparatus illustrated in **Figure 4.1** (Sato et al., 2006). The rotating speed of the rotor was 3000 rpm and the total milling time was 120 min.

Phase evolution during the milling was examined by XRD measurement (JDX-3530M, JEOL, Japan) using Ni filtered CuKα radiation as X-ray source. The XRD patterns were collected in the range of 10-70º with a step size of 0.02º. The specific surface areas (SSA) of the starting and the milled powder mixtures were measured with a nitrogen gas adsorption instrument (Micromeritics ASAP 2010, Shimadzu, Japan) based on the BET method with sample mass of about 2 g. The powder mixtures were dried at 200 ºC for 12 h before the SSA measurement. The morphology of the LSM powder was observed by scanning electron microscopy (SEM, ERA-8800FE, Elionics, Japan).

6.3 Results and Discussion

Figures 6.1 and 6.2 show the phase evolution of the powder mixture as a function of the milling time, the moisture contents of the starting powder mixture being < 0.2 and 0.8 wt. %, respectively. The phase evolutions in both cases exhibited similar behavior. Peaks of the individual starting powders, La_2O_3, $SrCO_3$ and Mn_3O_4, were clearly observed before the milling. After milling for 10 min, the peak intensities of the starting powders slightly decreased. After milling for 20 min, the peak intensities of the starting powders decreased further. In addition, the peaks corresponding to the LSM started to appear. This suggests that the mechanical forces

applied by milling were utilized efficiently for the formation of LSM during the first 20 min. After that continued milling reduced the peak intensities of the starting powders. Single phase LSM was successfully obtained after milling for 120 min.

In a third case in which the water content of the starting powder mixture was 2.0 wt.%, although disordering of the starting crystalline powders rapidly proceeded, single phase LSM was not obtained even after the powder mixture was milled for 120 min, as shown in **Figure 6.3.** It should be noted that the peaks identified as $La(OH)_3$ appeared at the start and at 10 min of milling. The formation of $La(OH)_3$ was effected by the hydration of La_2O_3 during humidification of the starting powder.
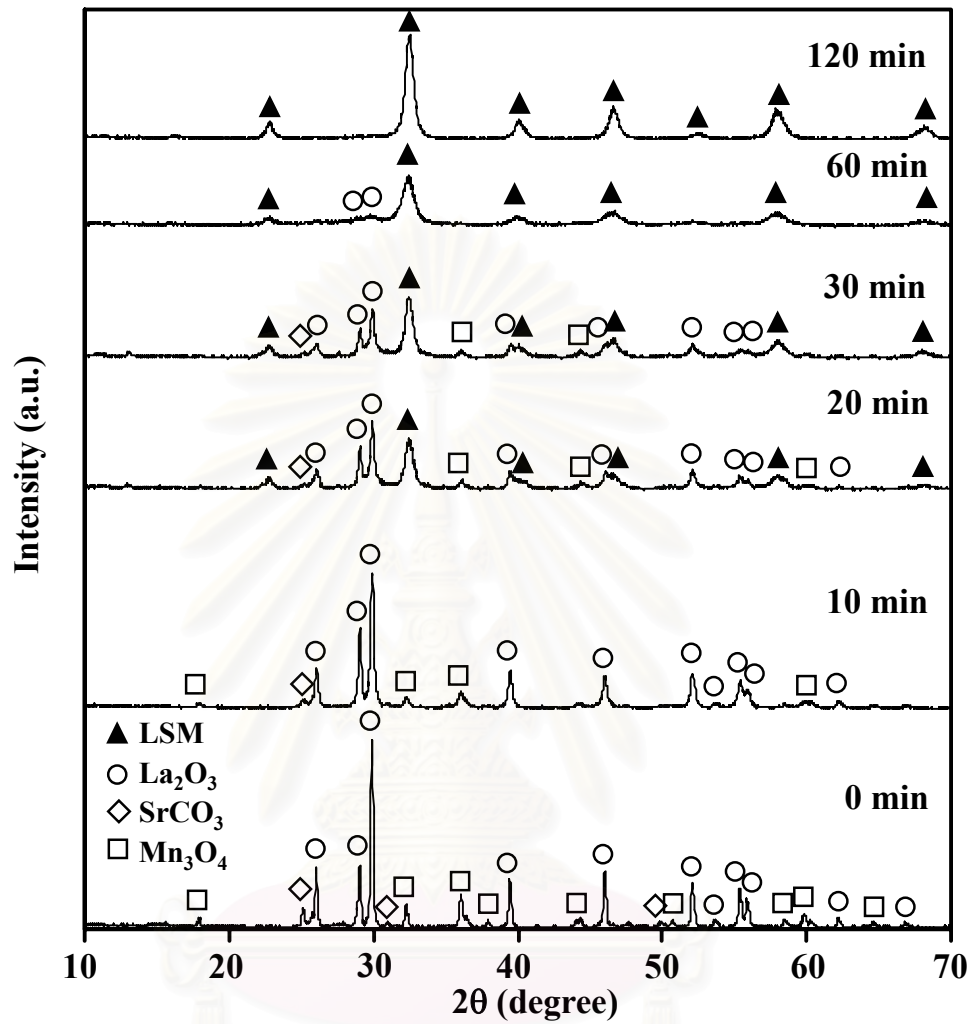
Figure 6.1 XRD patterns of the starting and milled powder mixtures: water content of starting powder mixture < 0.2 wt.%.
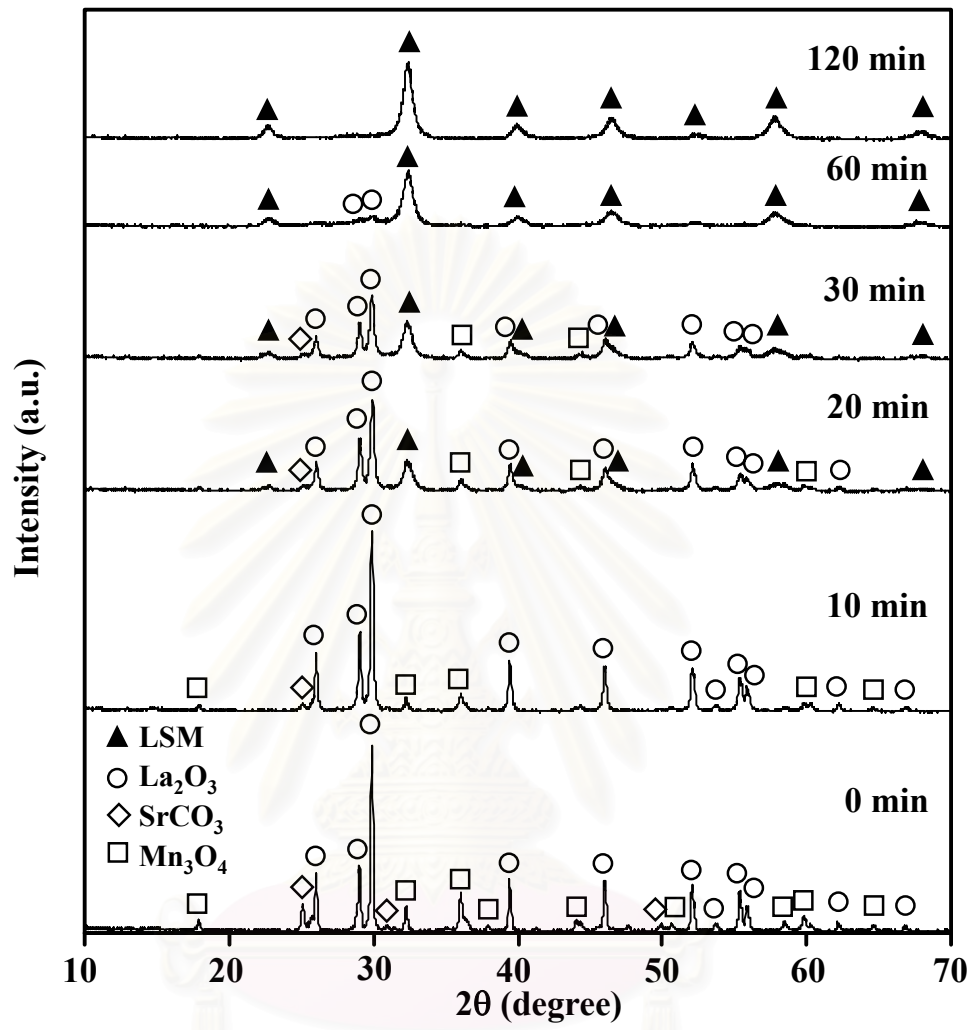
Figure 6.2 XRD patterns of the starting and milled powder mixtures: water content of starting powder mixture = 0.8 wt.%.
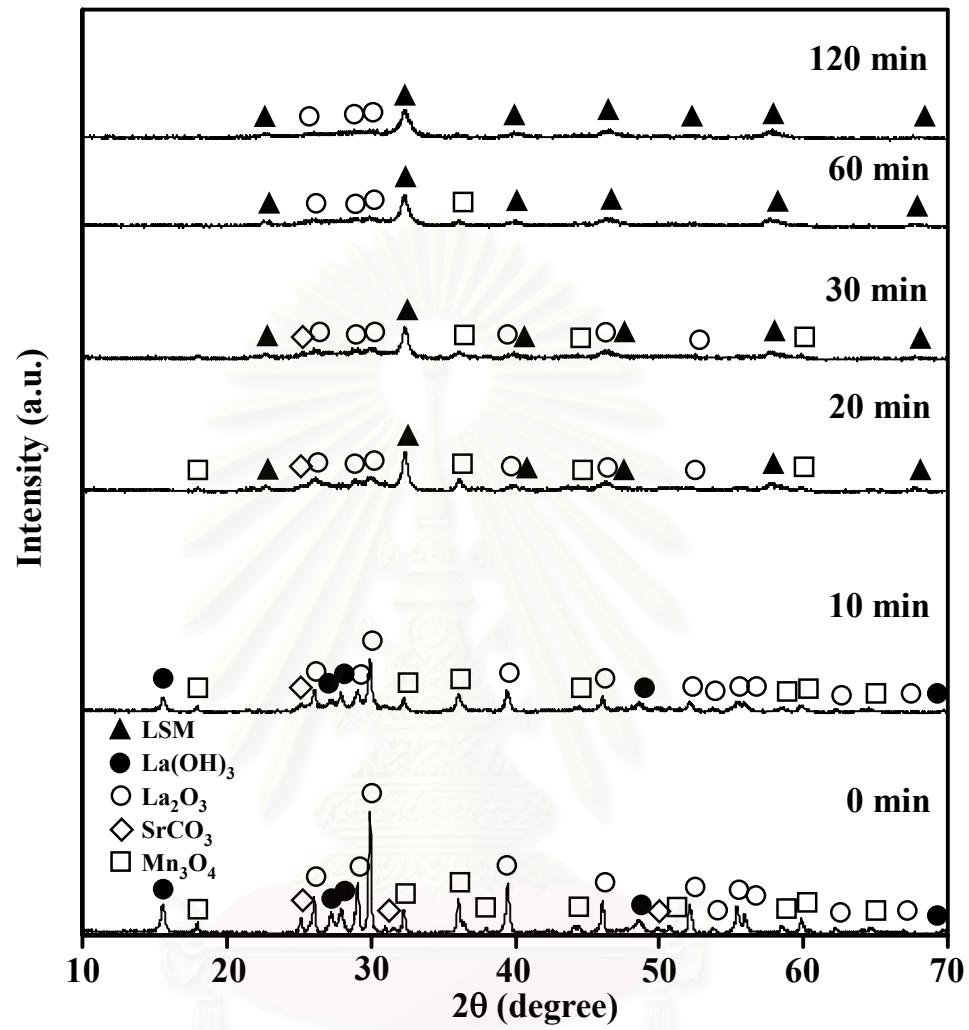
Figure 6.3 XRD patterns of the starting and milled powder mixtures: water content of starting powder mixture = 2.0 wt.%.

Figure 6.4 shows the change in the SSA of the powder mixture as a function of the milling time. The result shows that the SSA of all cases increased after 10 min of the milling. Then, the SSA gradually decreased after milling for 20 min. The results imply that the mechanical forces applied by milling contributed to the fine grinding of the powder mixture during the first 10 min of milling, resulting in significant increase in the SSA. The rapid formation of the LSM can be attributed to the intimate microscopic mixing achieved during the early stage of the milling. In the case of water content lower than 0.2 wt.%, the SSA again increased after milling for 30 min, then there was no significant change until 60 min. It significantly increased after milling for 120 min. A similar behavior has been reported on the synthesis of LSM powder by milling constituent oxides of La_2O_3-SrO-Mn_2O_3-MnO_2 in dry condition (Zhang, Nakagawa and Saito, 2000). When the initial water content was 0.8 wt.%, the SSA did not significantly change after further milling for 30-120 min. On the other hand, at 2.0 wt.% initial water content, the prolonged milling resulted instead in a significant decrease of the SSA.

As mentioned in section 4.3.1, after the SSA reached a maximum (around 10 min), the peaks corresponding to the LSM on the XRD patterns appeared and those of the starting powders significantly decreased. This confirms that the increase of the SSA and the disordering of crystalline structures of the raw substances were of vital importance for solid state reaction of LSM in the present milling. In this case, the presence of proper water content in the starting powder is shown to be an important factor. La_2O_3 is easily hydrated in the presence of water vapor, while Mn_3O_4 and $SrCO_3$ are not. Generally, the mechanical hardness of metal hydroxides is significantly lower than that of their corresponding oxides. Therefore, the Mn_3O_4 and

$SrCO_3$ powders would act as media balls and preferentially ground out the $La(OH)_3$ formed on the surface of La_2O_3 powder, thereby resulting in an increase of the SSA. Consequently, a large area of contacts between the reactant substances would be achieved. Such a microscopic mixing state would promote the solid state reaction of LSM. However, after mechanochemical reaction, the excess water in the starting powder worked as a binder combining the fine particles into agglomerates and merged into large particles (Zhang et al., 2002). In the present case, it is obvious that, when the water content of the starting powder increased to 2.0 wt.%, the SSA decreased as the milling time increased. No single phase LSM was obtained. This result implies that strong agglomeration has taken place rather than the mechanochemical reaction.

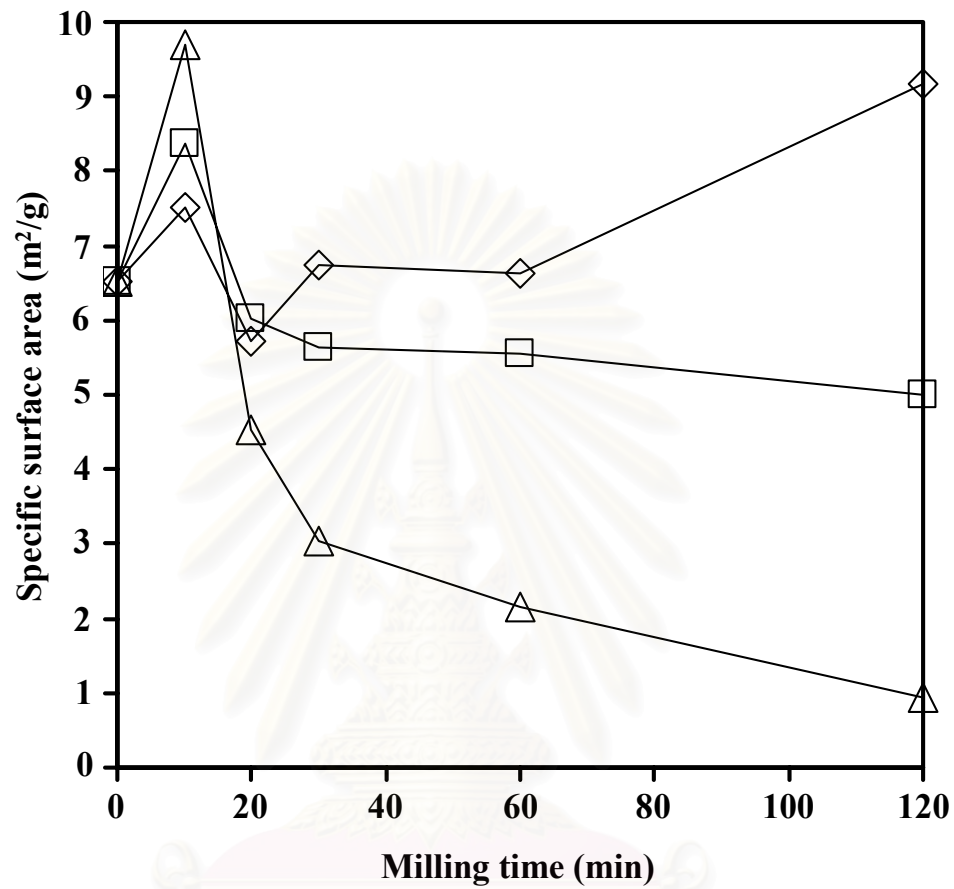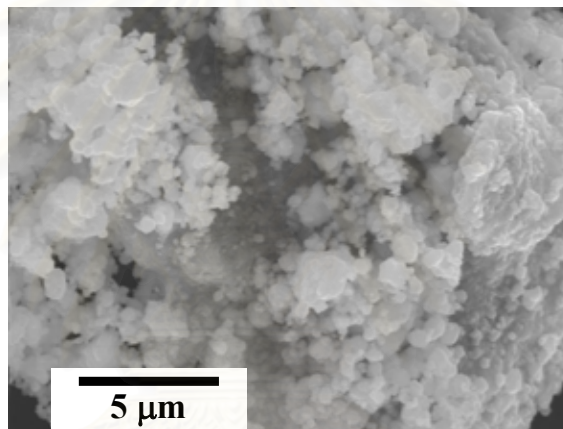**Figure 6.4** Specific surface area (SSA) of the starting and milled powders.

Water content

◇ < 0.2 wt%

☐ 0.8 wt%
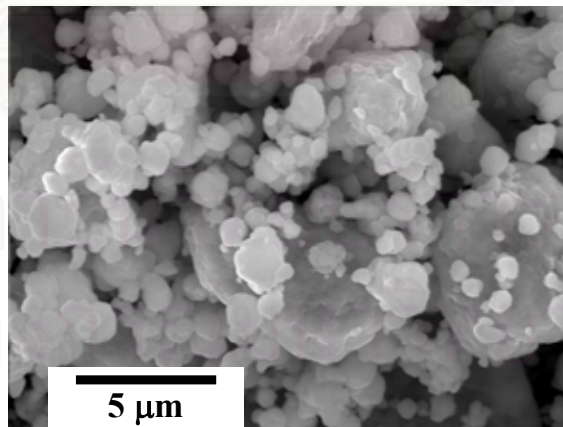
△ 2.0 wt%
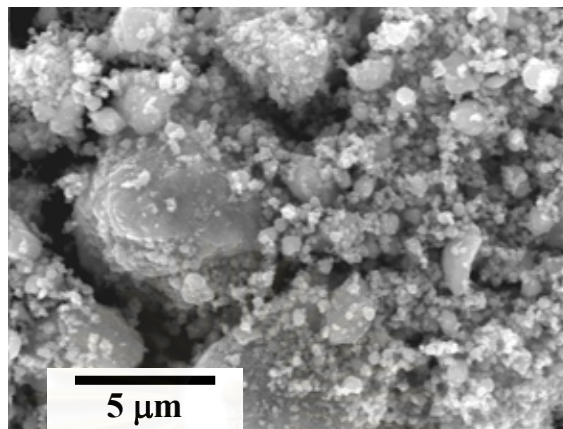
(a) Water content < 0.2 wt.%

(b) Water content = 0.8 wt.%

(c) Water content = 2.0 wt.%

Figure 6.5 SEM micrograph of LSM powder synthesized by milling powder mixture

for 120 min

Figure 6.5 shows SEM micrographs of the products synthesized by mechanical milling for 120 min. When the water contents were less than 0.8 wt.% (**Figure 6.5 (a) and (b)**), the milling products seemed to be agglomerates. These agglomerates consisted of fine primary particles about several hundred nanometers in size. In contrast, strong agglomeration was observed at water content about 2.0 wt.% (**Figure 6.5 (c)**). The size of the resulting primary particles observed in the micrograph was about 1 μm. These results confirm that the formation of large particles may be ascribed to the excess water content in the starting powder mixture. At two proper water contents, less than 0.2 and 0.8 wt.%, the specific surface area (SSA) of the LSM was 9.2 and 5.0 m^2/g, respectively. Their particle size calculated from the SSA was approximately 100 and 180 nm, respectively.

6.4 Conclusion

The influence of the water content of the starting powder mixture on the mechanochemical synthesis of $La_{0.8}Sr_{0.2}MnO_3$ (LSM) powder was investigated. Industrial-grade La_2O_3, $SrCO_3$ and Mn_3O_4 powders were used as staring materials. The water content of the starting powder mixture was varied up to 2.0 wt.%. At the water content of 2.0 wt.%, disordering of the starting crystalline powders rapidly proceeded while strong agglomeration was observed. However, single phase LSM powder was not obtained. At the two proper water contents (less than 0.2 wt.% and 0.8 wt%), fine grinding of the mixture occurred at an early stage of the milling and single phase LSM powder was obtained after 120 min of milling. The specific surface area (SSA) of the LSM was 5.0 m^2/g and the particle size calculated from the SSA was about 180 nm.

CHAPTER VII

INFLUENCE OF SIZE DISTRIBUTIONS OF LSM/YSZ

COMPOSITE POWDERS ON THE MICROSTRUCTURE

AND PERFORMANCE OF SOFC CATHODE

7.1 Introduction

Over the last two decades, SOFCs based on Y_2O_3 stabilized ZrO_2 (YSZ) have been developed for operation in a temperature range of 900-1000°C (Jørgensen et al., 2001; Jiang and Wang, 2005). More specifically, YSZ is used for the electrolyte, Ni-YSZ cermet for the anode, and $La_{0.8}Sr_{0.2}MnO_3$ (LSM) for the cathode. Current efforts are aimed at decreasing the operating cost of SOFC by lowering the operating temperatures to 800 °C or less. To achieve this purpose, the ohmic loss from the electrolyte should be minimized, while the polarization losses at both electrodes should further be decreased (Choi et al., 2000; Leng et al., 2003; Fukui, 1997). To date, the change in cell design and the improvement of powder processing have resulted in significant decreases of these losses for lab-scale planar SOFCs. The polarization losses at both electrodes can be reduced by increasing their electrochemical activity (Minh, 1993). Since electrochemical reaction takes place at triple phase boundaries (TPB) where gaseous species, ions and electrons must be coincident, a microstructure with large TPB leads to a decrease in the polarization loss. Therefore the microstructural control of anode or cathode electrode has become the objective of this investigation.

Recently, Fukui et al. (2004) have demonstrated that Ni/YSZ composites made from NiO-YSZ composite particles can provide large TPB, and thereby substantially decrease the polarization loss of the anode electrode. As for the cathode, the LSM/YSZ composites have been attempted as well (Fukui et al., 2001). As widely accepted, not only the processing conditions but also the powder characteristics such as particle size distributions (PSD) are important factors to obtain well-controlled microstructures. However, elucidation of PSD influence on the performance of SOFCs has been rather limited.

In this study, control of the microstructure of the LSM/YSZ cathode was attempted by varying the compounding method or the processing time to obtain LSM/YSZ composite particles. More specifically, the effect of the particle size distribution and microstructure of LSM/YSZ composites on the losses by internal resistance and polarization of the cathode was investigated.

7.2   Experimental

7.2.1 Synthesis of LSM-YSZ composite powder

Figure 7.1 shows a process flow diagram for the preparation of the LSM/YSZ composite particles used in this study. La_2O_3 (KCM Corp., Japan), $SrCO_3$ (KCM Corp., Japan) and Mn_3O_4 (KCM Corp., Japan) powders were milled for 60 min prior to calcining and holding at 800 ^{o}C for 1 h. Next, the synthesized LSM powder was ground by ball milling in ethanol for 12 h in order to disintegrate the agglomeration of the synthesized powder. After drying, the LSM powder was mixed with YSZ (TZ-8Y, Tosoh Inc., Japan) by an advanced mechanochemical process (Sato et al., 2006) to

make composite particles. The weight ratio of LSM to YSZ was 7:3. LSM/YSZ-1 and LSM/YSZ-2 are the composite particles obtained by using processing time of 10 and 30 min, respectively. In addition, the composite powder obtained after 12 hr ball-milling in ethanol is referred as LSM/YSZ-3.

The specific surface of the composite powders was measured by a nitrogen gas adsorption instrument (Micromeritics ASAP 2010, Shimadzu, Japan) based on the BET method. The composite powders were dried at 200 ^{o}C for 12 h before the SSA measurement. The particle size distribution (PSD) of the composite powders was measured by the laser diffraction method (MICROTRAC, Model HRA9320-X100, NIKKISO Co. Ltd., Japan). The composite powders were dispersed in ethanol by a homogenizer before the PSD measurement. The morphology of LSM/YSZ powders was observed via scanning electron microscopy (SEM, Model S-3500N, Hitachi Ltd., Japan). Phase identification of the composite powders was determined with the X-ray diffraction method (XRD: JDX-3530M, JEOL, Japan) using CuKα radiation as X-ray source. The XRD patterns were collected in the range of 10-70º with a step size of 0.02º.
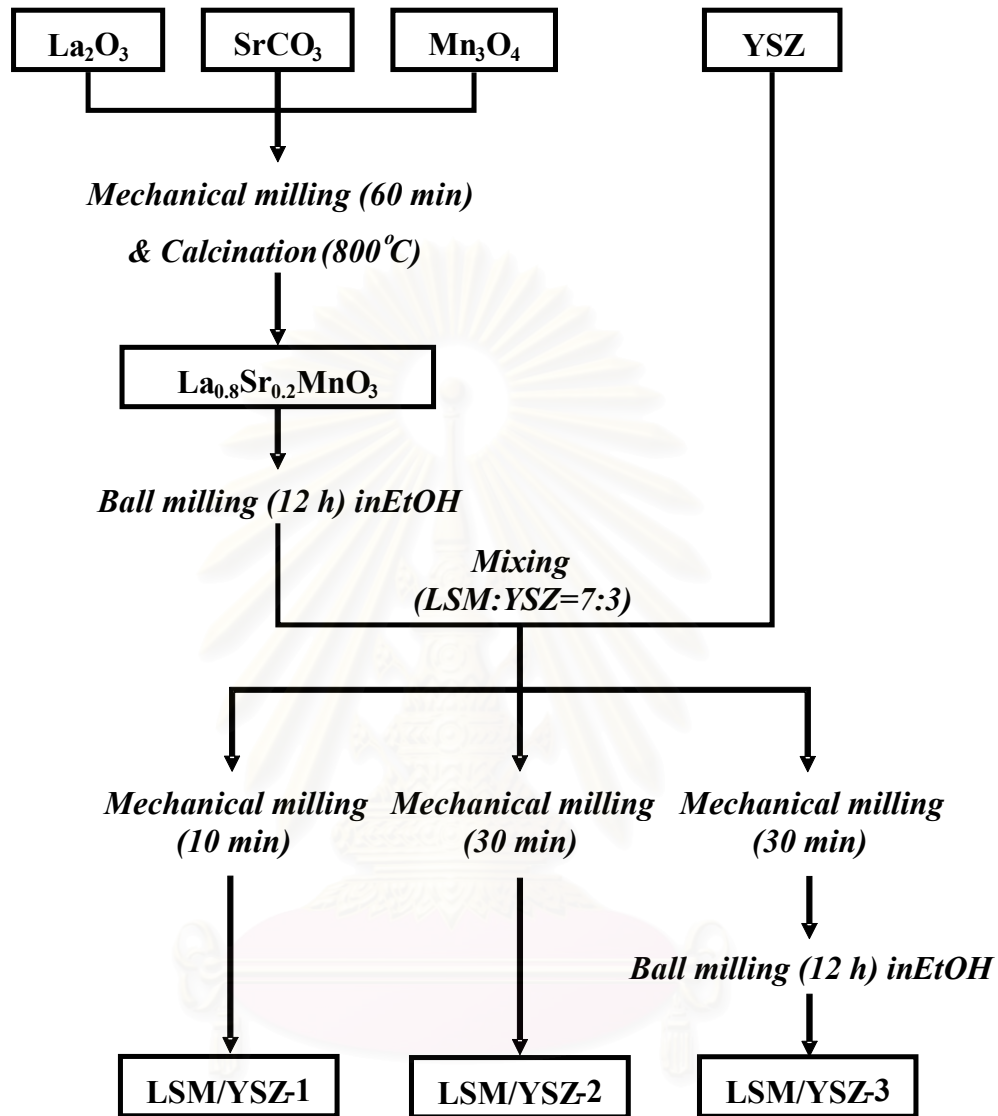
Figure 7.1 Process flow diagram for making LSM/YSZ composite particles

7.2.2 Fabrication and testing of SOFC

The electrolyte sheet was prepared from the YSZ powder (TZ-8Y, Tosoh Inc., Japan). The NiO (Nicoh Rita Corp, F-Type)-YSZ composite powders (Fukui et al., 2004; Murata et al., 2004) were mixed with an organic binder, and then printed onto a face of the YSZ electrolyte pellet before being sintered at 1350 $^{\circ}$C. The LSM/YSZ

composite particles were printed on the other face of the electrolyte pellet, and then sintered at 1150 $^{\circ}$C. The losses of internal resistance (IR) and polarization between the YSZ electrolyte layer and the cathode were measured using the current interruption technique as shown in **Figure 7.2**, with current density up to 0.5 A/cm^2 at the operating temperature of 700 $^{\circ}$C while supplying H$_2$ - 3%H$_2$O to the anode and air to the cathode. The microstructure of the cathode was analyzed with the SEM (Model S-3500N, Hitachi Ltd., Japan). The fabrication and testing of solid oxide fuel cell was conducted by Hosokawa Powder Technology Research Institute.
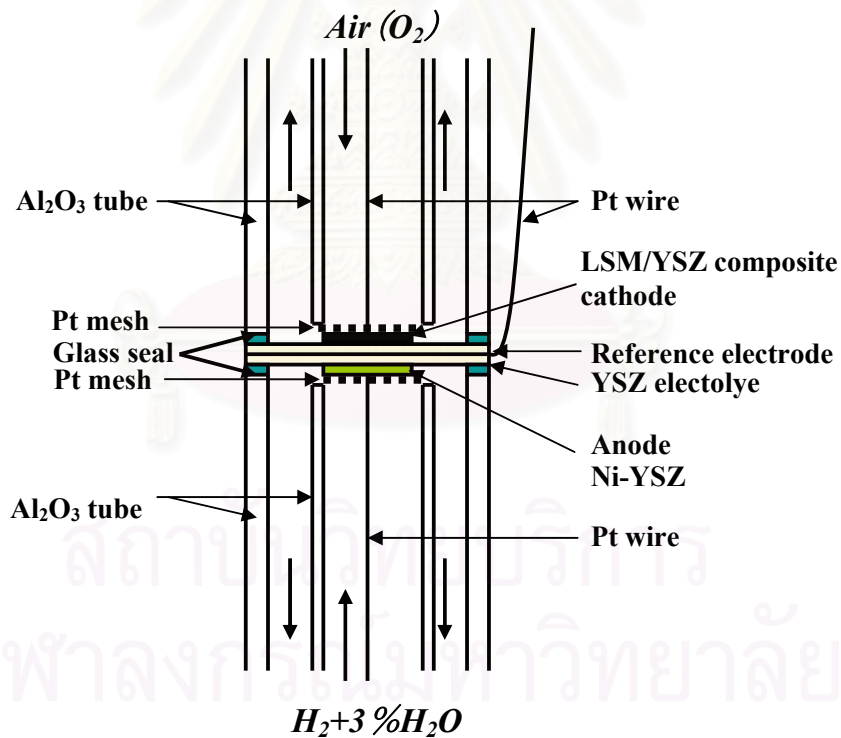

Figure 7.2 Schematic illustration of SOFC testing apparatus (Hosokawa Powder Technology Research Institute).

7.3   Results and Discussion

7.3.1   Powder Characterization

Figure 7.3 shows the SEM micrographs of the three LSM/YSZ composite powders, whose the particle size distributions are shown in **Figure 7.4**. Interestingly, LSM/YSZ-1 (D_{50}=0.45μm) and LSM/YSZ-3 (D_{50}=0.37μm) powders exhibit a bimodal distribution ranged that from 0.1 μm to a few micrometers. Meanwhile, LSM/YSZ-2 (D_{50}=6.49μm) reveals a much broader size distribution ranging from 0.1 to 100 μm.   However, BET analyses reveal that the specific surface areas of LSM/YSZ-1, LSM/YSZ-2 and LSM/YSZ-3 were 8.7, 8.1 and 10.9 m^2/g, respectively.

Figure 7.5 shows the XRD patterns of the three composite powders. Though LSM and YSZ phases could be identified, insignificant zirconate phases were observed.

7.3.2   Microstructure and Performance of LSM/YSZ Composite Cathode

Figure 7.6 shows some SEM micrographs of the surface of the LSM/YSZ composite cathodes. The SEM micrographs in **Figure 7.7** reveal the cross section of the electrolyte/cathode interface. The microstructure of the composite cathode made from LSM/YSZ-2 powders consisted of coarse grains and non-uniform porosity, suggesting a low effective area for the electrochemical reactions. Relatively coarse grains and large pores were observed close to the interfaces between the cathode and electrolyte, suggesting a small contact area, which in turn was expected to result in an increase of IR loss. On the other hand, the microstructures of the cathodes made from LSM/YSZ-1 and LSM/YSZ-3 powders consisted of smaller particles and more
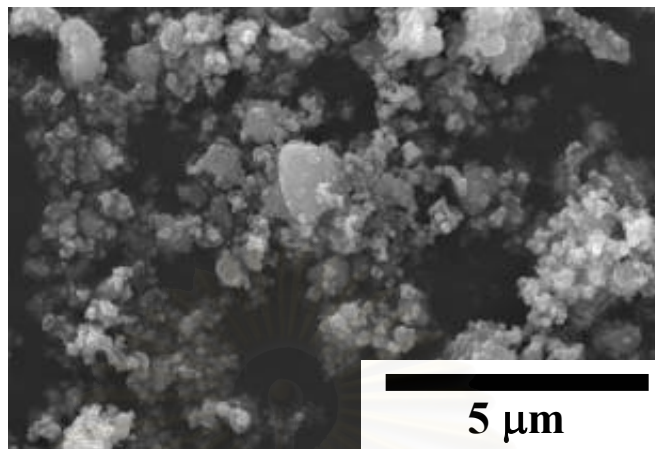
uniform porous structure. Good contacts between the electrolyte and the cathode were also observable.

   Figure 7.8 shows the losses by IR between the electrolyte layer and the cathode as well as that due to cathode polarization. Both IR and polarization losses, respectively, exhibited the highest value of 1.2 and 0.6 V when LSM/YSZ-2 composite particles were used. Meanwhile the cathodes made from LSM/YSZ-1 and LSM/YSZ-3 showed insignificant differences in both losses. This result implies that LSM/YSZ particles with broader size distribution led to a larger amount of coarse particles and less uniform microstructure, thereby showing less contacts within the electrolyte layer. Therefore, the IR and polarization losses of the cathode were negatively affected by the increasing content of coarse particles. This performance is similar to a previous report (Murata et al., 2005) in which the cathode polarization was reduced when the cathode exhibited a finer and more homogeneous microstructure with fine grain size. The reduction of the overall cathode polarization might be caused by a microstructure which presents a higher surface area for O_2 reduction reaction and a better transportation of gaseous species through a uniform porous structural cathode. As mentioned in section 7.1, the polarization losses at the cathode can be reduced by increasing their electrochemical activity. Since electrochemical reaction takes place at triple phase boundaries (TPB) which determine the activation polarization, a microstructure with large TPB leads to a decrease in the activation polarization loss. In addition, the concentration polarization is influenced by the transport of gaseous species through the cathode (Zhao and Virkar, 2005). Finally, optimization of the particle size distribution of the composite
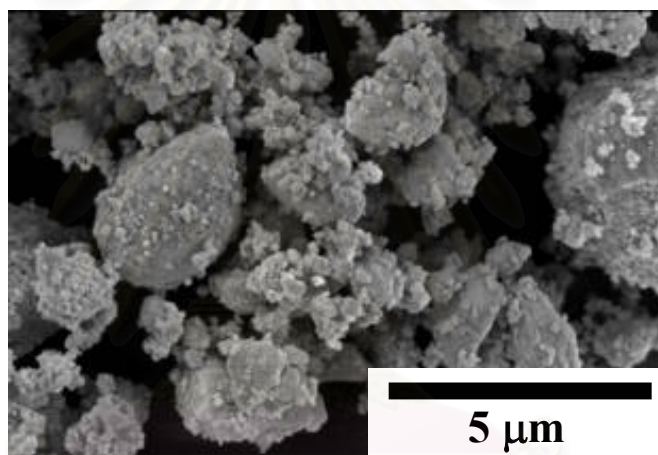
powder should be carried out because it plays an important role in the cathode performance.

(a) LSM/YSZ-1

(b) LSM/YSZ-2
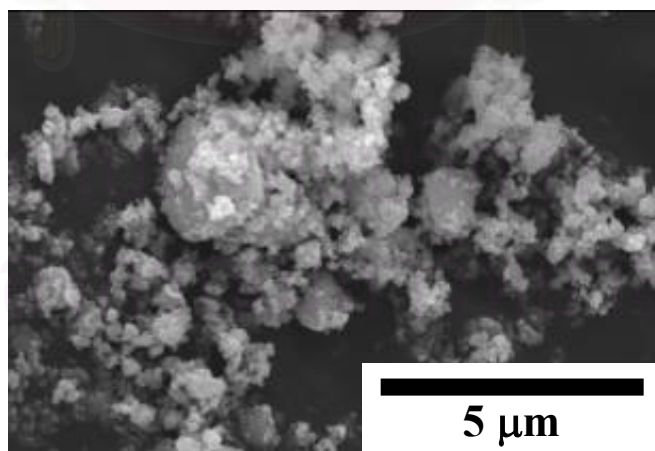
(c) LSM/YSZ-3

Figure 7.3 SEM micrographs of LSM/YSZ composite particles

Figure 7.4 Particle size distributions of LSM/YSZ composite particles

Figure 7.5 XRD patterns of LSM/YSZ powders

สถาบันวิทยบริการ
จุฬาลงกรณ์มหาวิทยาลัย
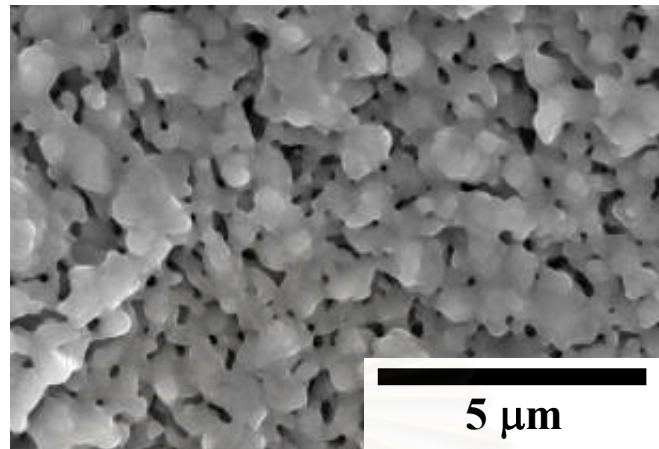
(a) LSM/YSZ-1
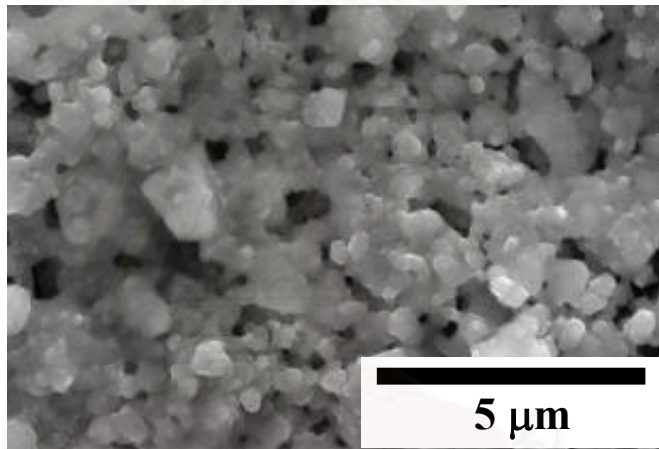
(b) LSM/YSZ-2
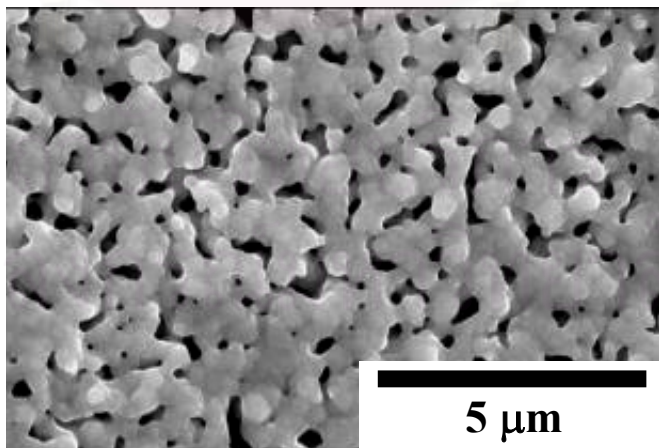
(c) LSM/YSZ-3

Figure 7.6 SEM micrographs of the surface of LSM/YSZ cathodes
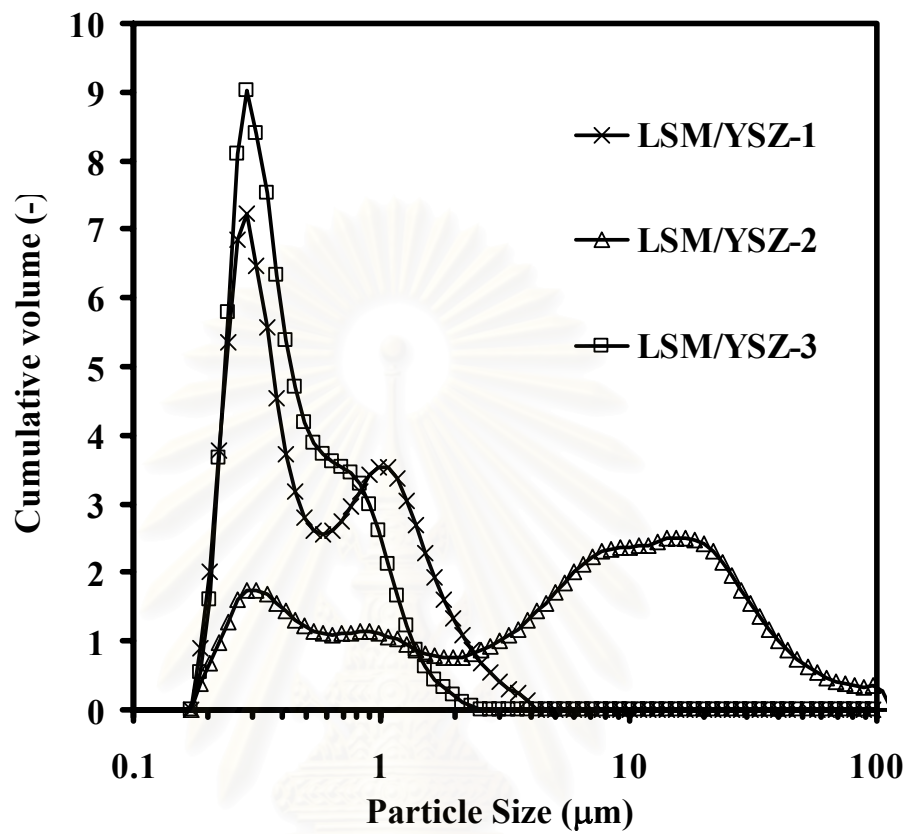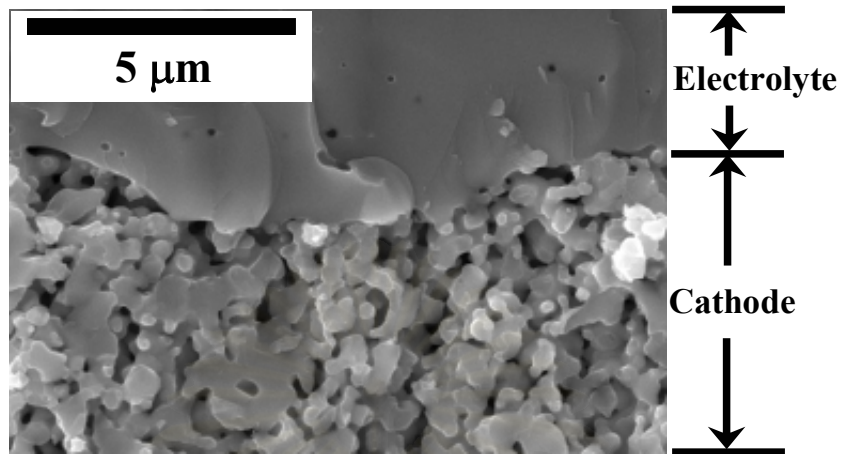
(a) LSM/YSZ-1
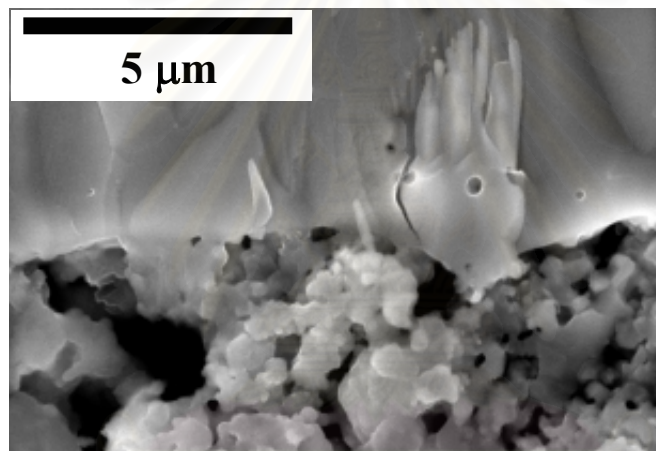
(b) LSM/YSZ-2
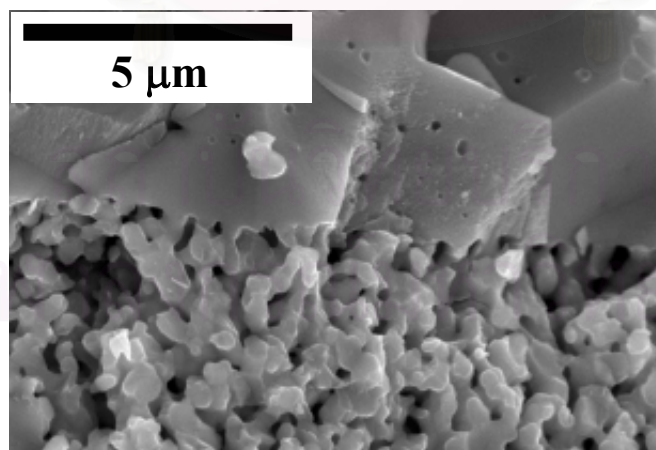
(c) LSM/YSZ-3

Figure 7.7 SEM micrographs of the cross-section of LSM/YSZ cathodes
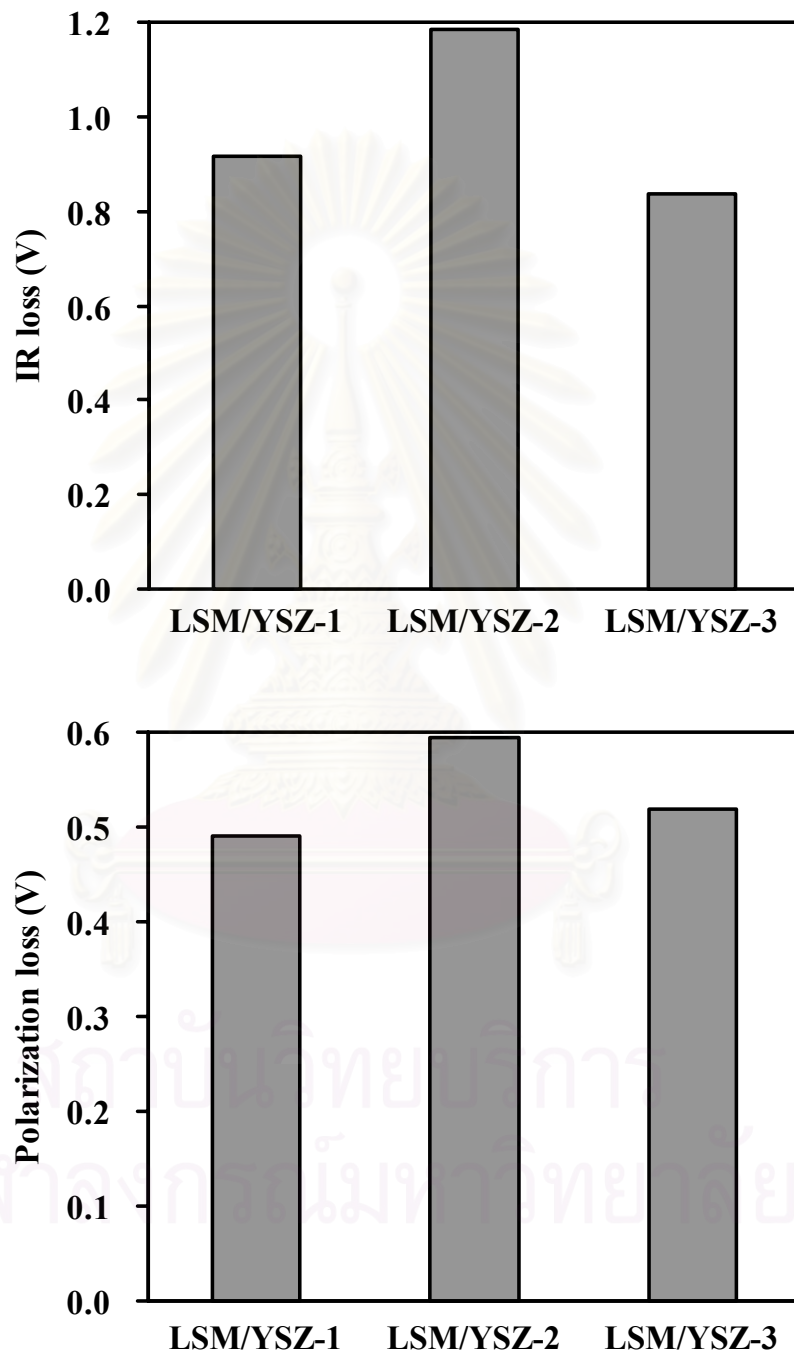
Figure 7.8 Losses of internal resistance (IR) and polarization of the LSM/YSZ composite cathodes at 0.5 A/cm^2, 700 $^{\circ}$C

7.4 Conclusion

The influence of particle size distribution of the LSM/YSZ composite particles on the microstructure, the internal resistance (IR) and the polarization loss of the cathode of a solid oxide fuel cell (SOFC) was investigated. In this study, LSM/YSZ composite particles with three different particle size distributions were prepared. The cathode fabricated by using the composite particles with narrow particle size distribution showed the fine grains, uniform porous structure, and good contact within the electrolyte layer, and thereby it showed low IR and polarization losses. In contrast, the cathode fabricated from the composite particles containing large amount of coarse particles occupied a non-uniform structure in grains and pore structure, resulting in high IR and polarization losses. Therefore, to control the particle size distribution of the LSM/YSZ composite powder, its important role in regulating higher performance of the cathodes could be confirmed.

CHAPTER VIII

CONCLUSIONS AND RECOMMENDATIONS

8.1 Conclusions

8.1.1 Phase Evolution of Lanthanum Strontium Manganite ($La_{0.8}Sr_{0.2}MnO_3$) During Milling by Advanced Mechanochemical Process

Mechanical milling of a powder mixture of industrial-grade La_2O_3, $SrCO_3$ and Mn_3O_4 powders was conducted under a humid atmosphere (RH 70% at 25 $^\circ$C). An attrition type milling apparatus without any media balls was used, thereby providing the mechanical activation through frictions among particles during the milling. The XRD peak intensities of La_2O_3, $SrCO_3$ and Mn_3O_4 decreased, and the specific surface area of the powder mixture increased in the early stage of the milling (<10min). After milling for 20 min, the lanthanum strontium manganite (LSM) started to appear. Additional milling further reduced the peak intensities of the starting powders. However, the intensity of LSM remained almost constant. DTA analysis revealed that the use of the present mechanical activation accelerated the decomposition of $SrCO_3$ and the phase change of Mn_3O_4.

8.1.2 Low Temperature Synthesis of Lanthanum Strontium Manganite ($La_{0.8}Sr_{0.2}MnO_3$) by Advanced Mechanochemical Process

Formation of lanthanum strontium manganite (LSM) was observed after only 20 min of milling without any heating. The rapid formation of LSM can be attributed to the intimate microscopic mixing achieved during the early stage of the milling. The influence on the synthesis temperature of LSM was also investigated. Single phase LSM was obtained by heating and holding the powder mixture milled for 60 min at 900 °C for 6 hours. The lower synthesis temperature, when compared to the conventional solid state process, is attributed to the mechanical activation of the advanced mechanochemical process. A short milling time of 60 min and a low synthesis temperature of 900 °C resulted in fine LSM particles with the average particle size of 90 nm. The advanced mechanochemical process without ball media and with short milling time brings an additional advantage of lower Fe contamination compared with the other mechanical methods.

8.1.3 Influence of the Water Content of the Starting Powder Mixture on the Mechanochemical Synthesis of Lanthanum Strontium Manganite

The influence of the water content of the starting powder mixture on the mechanochemical synthesis of $La_{0.8}Sr_{0.2}MnO_3$ (LSM) powder was investigated. Industrial-grade La_2O_3, $SrCO_3$ and Mn_3O_4 powders were used as starting materials. The water content of the starting powder mixture was varied up to 2.0 wt.%. At water content of 2.0 wt.%, disordering of the starting crystalline powders rapidly proceeded. However, single phase LSM powder was not obtained. At the two proper water contents (less than 0.2 and 0.8 wt.%), fine grinding of the mixture occurred at the

early stage of the milling and single phase LSM powder was obtained after 120 min of milling. The specific surface area (SSA) of the LSM was 5.0 m^2/g and the particle size calculated with the SSA was about 180 nm.

8.1.4 Influence of Size Distributions of LSM/YSZ Composite Powders on the Microstructure and Performance of SOFC Cathode

The influence of particle size distribution of the LSM/YSZ composite particles on the microstructure, the internal resistance (IR) and the polarization loss of the cathode of a solid oxide fuel cell (SOFC) was investigated. In this study, LSM/YSZ composite particles with three different particle size distributions were prepared. A cathode fabricated from composite particles with narrow particle size distribution showed fine grains, uniform porous structure, and good contact within the electrolyte layer, and therefore it showed low IR and polarization losses. In contrast, a cathode fabricated from composite particles containing large amount of coarse particles exhibited a non-uniform structure in grains and pore structure, resulting in high IR and polarization losses.

8.2 Recommendations for Future Work

- The micro mixing state required to trigger the solid state reaction should further be investigated with TEM-EDS tools.
- The valence change associated with the mechanochemical synthesis should be investigated further.
- Optimization of the particle size distribution of the composite powder should be carried out because it plays an important role in the cathode performance.

REFERENCES

Algueró, M.; Ricote, J.; and Castro A. Mechanosynthesis and thermal stability of piezoelectric perovskite $0.92Pb(Zn_{1/3}Nb_{2/3})O_3$-$0.08PbTiO_3$ powders. <u>J. Am. Ceram. Soc.</u> 87[5] (2004): 772-778.

Avvakumov, E.G., Soft mechanochemical synthesis as a basis for new chemical processes. <u>Chem. Sustain. Dev.</u> 2 (1992): 1-15.

Avvakumov, E.G. Soft mechanochemical synthesis as a basis for new chemical technologies. <u>Chem. Sustain. Dev.</u> 2 (1994): 541-558.

Baek J.,-G.; Isobe, T.; and Senna, M. Mechanochemical effects on the precursor formation and microwave dielectric characteristics of $MgTiO_3$. <u>Solid State Ionics</u> 90[9] (1996): 269-279.

Barbucci, A.; Viviani, M., Panizza, M.; Delucchi, M.; and Cerisola, G. Analysis of the oxygen reduction process on SOFC composite electrodes. <u>J. App. Electrochem.</u> 35 (2005): 399-403.

Bell, R.; Millar, G.J.; and Drennan, J. Influence of synthesis route on the catalytic properties of $La_{1-x}Sr_xMnO_3$. <u>Solid State Ionics</u> 131 (2000): 211-220.

Berbenni, V.; Marini, A.; and Bruni, B. Effect of mechanical activation on the preparation of $SrTiO_3$ and Sr_2TiO_4 ceramics from the solid state system $SrCO_3$-TiO_2. <u>J. Alloys and Comp.</u> 329 (2001): 230-238.

Brant, M.C.; and Dessemond, L. Electrical degradation of LSM-YSZ interfaces. <u>Solid State Ionics</u> 138 (2000): 1-17.

Cairns, D.L.; Reaney, I.M.; Zheng, H.; Iddles, D.; and Price, T. Synthesis and characterization of La(Co$_{1/2}$Ti$_{1/2}$)O$_3$. J. Eur. Ceram. Soc. 25 (2005): 433-439.

Charojrochkul, S.; Choy, K.L.; Steele, B.C.H. Flame assisted vapour deposition of cathode for solid oxide fuel cells. 1. Microstructure control from processing parameters. J. Eur. Ceram. Soc. 24 (2004): 2515-2526.

Charojrochkul, S.; Lotian, R.M.; Choy, K.L.; Steele, B.C.H. Flame assisted vapour deposition of cathode for solid oxide fuel cells. 2. Modelling of processing parameters, J. Eur. Ceram. Soc. 24 (2004): 2527-2535.

Chen, X.J.; Khor, K.A.; and Chan, S.H. Electrochemical behavior of La(Sr)MnO$_3$ electrode under cathodic and anodic polarization. Solid State Ionics 167 (2004): 379-387.

Choi, J.H.; Jang, J.H.; Ryu, J.H.; and Oh, S.M. Microstructure and cathodic performance of La$_{0.9}$Sr$_{0.1}$MnO$_3$ electrodes according to particle size of starting powder. J. Power Sources 87 (2000): 92-100.

Choy, K.; Bai, W.; Charojrochkul, S.; Steele, B.C.H. The development in intermediate-temperature solid oxide fuel cells for the next millennium. J. Power Sources 71 (1998): 361-369.

Fernández-Rodríguez, J.M.; Morales, J.; and Tirado, J.L. Synthesis and alteration of α-LiFeO$_2$ by mechanochemical processes. J. Mater. Sci. 23[8] (1988): 2971-2974.

Fritsch, S.; Sarrias, J.; Rousset, A.; and Kulkarni, G.U. Low-temperature oxidation of Mn$_3$O$_4$ Hausmannite. Mater. Res. Bull. 33 (1998): 1185-1994.

Fu, Z.Y.; and Wei, S.L. Mechanochemical activation of calcium oxide powder. Powder Technol. 87 (1996): 249-254.

Fukui, T.; Murata, K.; Ohara, S.; Abe, H.; Naito, M.; and Nogi, K. Morphology control of Ni–YSZ cermet anode for lower temperature operation of SOFCs. J. Power Sources 125 (2004): 17-21.

Fukui, T.; Ohara, S. Naito, M.; and Nogi, K. Morphology control of the electrode for solid oxide fuel cells by using nanoparticles. J. Nanopart. Res. 3 (2001): 171-174.

Fukui, T.; Oobushi, T.; Ikuhara, Y.; Ohara, S.; and Kodera, K. Synthesis of $(La,Sr)MnO_3$-YSZ composite particles by spray pyrolysis. J. Am. Ceram. Soc. 80[1] (1997): 261-263.

Fukunaga, H.; Ihara, M.; Sakaki, K.; and Yamada, K. The relationship between overpotential and the three phase boundary length. Solid State Ionics 86-88 (1996): 1179-1185.

Fukunaga, H.; Koyama, M.; Takahashi, T.; Wen, C.; and Yamada, K. Reaction model of dense $Sm_{.5}Sr_{.5}CoO_3$ as cathode. Solid State Ionics 132 (2000): 279-285.

Garcia-Martinez, G.; Martinez-Gonzalez, L.G.; Escalante-García, J.I.; and Fuentes, A.F. Phase evolution induced by mechanical milling in La_2O_3:TiO_2 mixtures (Ln=Gd and Dy). Powder Technol. 152 (2005): 72-78.

Gaudon, M.; Laberty-Robert, C.; Ansart, F.; Dessemond, L.; and Stevens, P. Evaluation of a sol-gel process for the synthesis of $La_{1-x}S_xMnO_{3+\delta}$ cathodic multilayers for solid oxide fuel cells. J. Power Sources 133 (2004): 214-222.

Gaudon, M.; Laberty-Robert, C.; Ansart, F.; Stevens, P.; and Rousset, A. Preparation and characterization of $La_{1-x}Sr_xMnO_{3+\delta}$ ($0 \leq x \leq 0.6$) powder by sol-gel processing. Solid State Sci. 4 (2002): 125-133.

Ghosh, D.; Martel, F.; and Tang, Z.; Composite electrodes for solid state devices. Patent No. US 6,750,169 B2 (2004).

Ghosh, A.; Sahu, A.K.; Gulnar, A.K.; and Suri, A.K. Synthesis and characterization of lanthanum strontium manganite. Scripta Materialia 52 (2005): 1305-1309.

Gillot, B.; El Guendouzi, M.; and Laarj, M. Particle size effects on the oxidation-reduction behavior of Mn_3O_4 hausmannite. Mater. Chem. Phys. 70 (2001): 54-60.

Grossin D.; and Noudem, J.G. Synthesis of fine $La_{0.8}Sr_{0.2}MnO_3$ powder by different ways. Solid State Sci. 6 (2004): 939-944.

Haanappel, V.A.C; Mertens, J.; Rutenbeck, D.; Tropartz, C.; Herzhof, W.; Sebold, D.; and Tietz, F. Optimization of processing and microstructural parameters of LSM cathodes to improve the electrochemical performance of anode-supported SOFCs. J. Power Sources 141 (2005): 216-226.

Hibino, T.; Suzuki, K.; Ushiki, K.; Kuwahara, Y.; and Mizuno, M. Ultra-fine grinding of $La_{0.8}Sr_{0.2}MnO_3$ oxide by vibration mill. Appl. Cat. A: General 145 (1996): 297-306.

Inagaki, T.; Miura, K.; Yoshida, H.; Maric, R.; Ohara, S.; Zhang, X.; Mukai, K.; and Fukui, T. High performance electrodes for reduced temperature solid oxide fuel cells with doped lanthanum gallate electrolyte II. $La(Sr)CoO_3$ cathode. J. Power Sources 86 (2000): 347-351.

Ito, T.; Zhang, Q.; and Saito, F. Synthesis of perovskite-type lanthanum cobalt oxide nanoparticles by means of mechanochamical treatment. Powder Technol. 143-144 (2004): 170-173.

Ivers-Tiffée, E., Weber, A.; and Herbstritt, D. Materials and technologies for SOFC-components. J. Eur. Ceram. Soc. 21 (2001): 1805-1811.

Jiang, S.P. Issue on development of (La,Sr)MnO$_3$ cathode for solid oxide fuel cells. J. Power Sources 194 (2003): 390-402.

Jiang, S.P.; and Love, J.G. Observation of structure change induced by cathodic polarization on (La,Sr)MnO$_3$ electrodes of solid oxide fuel cells. Solid State Ionics 158 (2003) 45-53.

Jiang, S.P.; and Wang, W. Sintering and grain growth of (La,Sr)MnO$_3$ electrodes of solid oxide fuel cells under polarization. Solid State Ionics 176 (2005): 1185-1191.

Jiang, S.P.; Zhang, J.-P.; and Föger, K. Chemical interactions between 3 mol% yttria-zirconia and Sr-doped lanthanum manganite. J. Eur. Ceram. Soc. 23 (2003): 1865-1873.

Jørgensen, M.J.; Primdahl, S.; Bagger, C.; and Mogensen, M. Effect of sintering temperature on microstructure and performance of LSM-YSZ composite cathodes. Solid State Ionics 139 (2001): 1-11.

Kim, S.D.; Hyun, S.H.; Moon, J.; Kim, J.-H., and Song, R.H. Fabrication and characterization of anode-supported electrolyte thin films for intermediate temperature solid oxide fuel cells. J. Power Sources 139 (2005): 67-72.

Kumar, A.; Devi, P.S.; Sharma, A.D.; and Maiti, H.S. A novel spray-pyrolysis technique to produce nanocrystalline lanthanum strontium manganite powder. J. Am. Ceram. Soc. 88[4] (2005): 971-973.

Laio, J.; and Senna, M. Enhanced dehydration and amorphization of $Mg(OH)_2$ in the presence of ultrafine SiO_2 under mechanochemical conditions. Thermochim. Acta 210 (1992): 89-102.

Laio, J.; and Senna M. Mechanochemical dehydration and amorphization of hydroxides of Ca, Mg and Al on grinding with and without SiO_2. Solid State Ionics 66[3-4] (1993): 313-319.

Laio, J.; and Senna, M. Crystallization of titania and magnesium titanate from mechanically activated $Mg(OH)_2$ and TiO_2 gel mixture. Mater. Res. Bull. 30[4] (1995): 385-392.

Lee, H.Y.; and Oh, S.M. Origin of cathodic degradation and new phase formation at the $La_{0.9}Sr_{0.1}MnO_3$/YSZ interface. Solid State Ionics 90 (1996): 133-140.

Lee, J.; Zhang, Q.; and Saito, F. Mechanochemical synthesis of lanthanum oxyfluoride from lanthanum oxide and lanthanum fluoride. J. Am. Ceram. Soc. 84[4] (2001): 863-865.

Leng, Y.J.; Chan, S.H.; Khor, K.A.; and Jiang, S.P. Effect of characteristics of Y_2O_3/ZrO_2 powders on fabrication of anode-supported solid oxide fuel cells. J. Power Sources 117 (2003): 26-34.

Leng, Y.J.; Chan, S.H.; Khor, K.A.; and Jiang, S.P. Development of LSM/YSZ composite cathode for anode-supported solid oxide fuel cells. J. App. Electrochem. 34 (2004): 409-415.

Minh, N.Q. Ceramic fuel cells. J. Am. Ceram. Soc. 76[3] (1993): 563-588.

Mitsuyasu, H.; Eguchi, K.; and Arai, H. Microscopic analysis of lanthanum strontium manganite/yttria-stabilized zirconia interface. Solid State Ionics 100 (1997): 11-15.

Mori, M.; Sammes, N.M.; and Tompsett, G.A. Fabrication processing condition for dense sintered $La_{0.6}AE_{0.4}MnO_3$ perovskites synthesized by the coprecipitation method (AE = Ca and Sr). J. Power Sources 86 (2000): 395-400.

Murata, K.; Fukui, T.; Abe, H.; Naito, and M.; Nogi, K. Morphology control of $La(Sr)Fe(Co)O_{3-a}$ cathodes for IT-SOFCs. J. Power Sources 145 (2005): 257-261.

Naito, M.; Kondo, A.; and Yokoyama, T. Applications of comminution techniques for the surface modification of powder materials. ISIJ Int. 33 (1993): 915-924.

Pang, G.; Xu, X.; Markovich, V.; Avivi, S.; Palchik, O.; Koltypin, Y.; Gorodetsky, G.; Yeshurun, Y.; Buchkremer, H.P.; and Gedanken, A. Preparation of $La_{1-x}Sr_xMnO_3$ nanoparticles by sonication-assisted coprecipitation. Mater. Res. Bull. 38 (2003) 11-16.

Prabhakaran, K.; Joseph, J.; Gokhale, N.M.; Sharma, S.C.; and Lal, R. Sucrose combustion synthesis of $La_xSr_{(1-x)}MnO_3$ ($x \leq 0.2$) powders. Ceram. Int. 31 (2005): 327-331.

Rambert, S., McEvoy, A.J.; and Barthel, K. Composite ceramic fuel cell fabricated by vacuum plasma spraying. J. Euro. Ceram. Soc. 19(1999): 921-923.

Revas Mercury. J.M.; De Aza, A.H.; Turrillas, X.; and Pena, P. The synthesis mechanism of $Ca_3Al_2O_6$ from soft mechanochemically activated precursors studied by time-resolved neutron diffraction up to 1000 ^{o}C. J. Solid States Chem. 177 (2004): 866-874.

Sato, K.; Chaichanawong, J.; Abe, H.; and Naito, M. Mechanical synthesis of LaMnO$_{3+\delta}$ fine powder assisted with water vapor. Mater. Lett. 60 (2006): 1399-1402.

Sato, K.; Uemura, M.; Kondo, A.; Abe, H.; Naito, M. and Nogi, K. Microstructural control of composite anode supported for intermediate temperature solid oxide fuel cells. Key Eng. Mater. (in press).

Senna, M. Incipient chemical interaction between fine particles under mechanical stress - a feasibility of producing advanced materials via mechanochemical route. Solid State Ionics 63-65 (1993): 3-9.

Senna, M. Grinding of mixture under mild condition for mechanochemical complexation. Int. J. Miner. Process 44-45 (1996): 187-195.

Shi, Y.; Ding, J.; and Yin, H. CeFe$_2$O$_4$ nanoparticles prepared by mechanochemical method. J. Alloys and Comp. 308 (2000): 290-295.

Singhal, S.C. Advances in solid oxide fuel cell technology. Solid State Ionics 135 (2000): 305-313.

Song, Z. Fuel processing for low-temperature and high-temperature fuel cells challenge, and opportunities for sustainable development in 21st century. Catal. Today 77 (2002): 17-49.

Stambouli, A.B.; and Traversa, E. Solid oxide fuel cells (SOFCs): a review of environmentally clean and efficient source of energy. Renew. Sustain. Energy Rev. 6 (2002): 433-455.

Steele, B.C.H.; and Heinzel, A. Materials for fuel cell technologies. Nature 414 (2001) 345-352.

Steele, B.C.H.; Hori, K.M.; and Uchino, S. Kinetic parameters influencing the performance of IT-SOFC composite electrodes. Solid State Ionics 135 (2000): 445-450.

Stöver, D.; Buchkremer, H.-P.; and Uhlenbruck, S. Processing and properties of the ceramic conductive multilayer device solid oxide fuel cell (SOFC). Ceram. Int. 30[7] (2004) 1107-1113.

Temuujin, T.; Okada, K.; and MacKenzie, K.J.D. Role of water in the mechanochemical reactions of MgO-SiO$_2$ systems. J. Solid State Chem. 138 (1998): 160-177.

Wang, S.; Jiang, Y.; Zhang. Y.; Yan, J.; and Li, W. Promoting effect of YSZ on the electrochemical performance of YSZ + LSM composite electrodes. Solid State Ionics 113-115 (1998): 291-303.

Wang, W.G.; and Mogensen, M. High-performance lanthanum-ferrite-based cathode for SOFC. Solid State Ionics 176 (2005): 457-462.

Watanabe, T.; Isobe, T.; and Senna, M. Mechanisms of incipient chemical reaction between Ca(OH)$_2$ and SiO$_2$ under moderate mechanical stressing: I: A solid state acid–base reaction and charge transfer due to complex formation. J. Solid State Chem. 122 (1996): 74-80.

Weber, A.; and Ivers-Tiffée, E. Materials and concepts for solid oxide fuel cells (SOFCs) in stationary and mobile applications. J. Power Sources 127 (2004): 273-283.

Wincewicz, K.C.; and Cooper, J.S. Taxonomies of SOFC materials and manufacturing alternatives. J. Power Sources 140 (2005): 280-296.

Wu, Q.-H.; Liu, M.; and Jaegermann, W. X-ray photoelectron spectroscopy of $La_{0.5}Sr_{0.5}MnO_3$. Mater. Lett. 59 [12] (2005): 1480-1483.

Yamahara, K.; Sholklapper, T.Z.; Jacobson, C.P.; Visco, S.J.; and Jonghe, L.C.D. Ionic conductivity of stabilized zirconia networks in composite SOFC electrodes. Solid State Ionics 176 (2005): 1359-1364.

Yamaji, K.; Kishimoto, H.; Xiong, Y.; Horita, T.; Sakai, N.; and Yokokawa, H. Performance of anode-supported SOFCs fabricated with electrophoric deposition techniques. Fuel cells Bull. 2004[12] (2004): 12-15.

Yang, C.-C.T.; Wei, W.J.; and Roosen, A. Electrical conductivity and microstructures of $La_{0.65}Sr_{0.3}MnO_3$-8 mol% yttria-stabilized zirconia. Mater. Chem. Phys. 81 (2003): 134-142.

Yang, C.-C.T.; Wei, W.J.; and Roosen, A. Reaction kinetics and mechanism between $La_{0.65}Sr_{0.3}MnO_3$ and 8 mol% yttria-stabilized zirconia. J. Am. Ceram. Soc. 87 [6] (2004): 1110-1116.

Yu, H.-C.; and Fung, K.-Z. Electrode properties of $La_{1-x}Sr_xCuO_{2.5-\delta}$ as new cathode materials for intermediate-temperature SOFCs. J. Power Sources 133 (2004): 162-168.

Zhang, Q.; Nakagawa, T.; and Saito, F. Mechanochemical synthesis of $La_{0.7}Sr_{0.3}MnO_3$ by grinding constituent oxides. J. Alloys and Comp. 308 (2000): 121-125.

Zhang, Q.; and Saito, F.; Mechanochemical synthesis of $LaMnO_3$ from La_2O_3 and Mn_2O_3 powders. J. Alloys and Comp. 297 (2000): 99-103.

Zhang, Q.; Lu, J.; and Saito, F. Mechanochemical synthesis of $LaCrO_3$ by grinding constituent oxides, Powder Technol. 122 (2002): 145-149.

Zhao, F.; Virkar, A. V. Dependence of polarization in anode-supported solid oxide fuel cell on various cell parameters. <u>J. Power Sources</u> 141 (2000): 79-95.

Zhu, B.; Yang, X.T.; Xu, J.; Zhu, Z.G.; Ji, S.J.; Sun, M.T.; and Sun, J.C. Innovative low temperature SOFCs and advanced materials. <u>J. Power Sources</u> 118 (2003): 47-53.

APPENDIX

LIST OF PUBLICATIONS

International Research Paper

1. **J. Chaichanawong**, K. Sato, H. Abe, K. Murata, T. Fukui, T. Charinpanitkul, W. Tanthapanichakoon, M. Naito, Formation of strontium doped lanthanum manganite ($La_{0.8}Sr_{0.2}MnO_3$) by mechanical milling without media balls, Advanced Powder Technology (in press).

2. **J. Chaichanawong**, K. Sato, H. Abe, K. Murata, T. Fukui, T. Charinpanitkul, W. Tanthapanichakoon, M. Naito, Low temperature synthesis of strontium doped lanthanum manganite ($La_{0.8}Sr_{0.2}MnO_3$) by advanced mechanochemical process, Smart Processing Technology, High Temperature Society of Japan, 1 (2006) 207-210.

3. K. Sato, **J. Chaichanawong**, H. Abe, M. Naito, Mechanical synthesis of $LaMnO_{3+\delta}$ fine powder assisted with water vapor, Materials Letters , 60 (2006) 1139-1402.

4. T. Misono, K. Murata, T. Fukui, **J. Chaichanawong**, K. Sato, H. Abe, M. Naito, SDC cermet anode fabricated from NiO-SDC composite powder for intermediate temperature SOFC, Journal of Power Sources 157 (2006) 754-757.

Domestic Research Paper

1. **J. Chaichanawong**, K. Sato, H. Abe, K. Murata, T. Fukui, W. Tanthapanichakoon, T. Charinpanitkul, M. Naito, Influence of size distributions of LSM/YSZ composite powders on microstructure and performance of SOFC cathodes. Transactions of JWRI, Japan 34[1] (2005) 55-59.

International Conference

1. **J. Chaichanawong**, K. Sato, H. Abe, K. Murata, T. Fukui, W. Tanthapanichakoon, T. Charinpanitkul, M. Naito, Low temperature synthesis of strontium doped lanthanum manganite ($La_{0.8}Sr_{0.2}MnO_3$) by advanced mechanochemical process, International Symposium on Smart Processing Technology (ISMPT), Suita, Osaka, Japan, November 14-15, 2005.

2. **J. Chaichanawong**, K. Sato, H. Abe, W. Tanthapanichakoon, T. Charinpanitkul, M. Naito, Influence of water content of starting powder mixture on the mechanochemical synthesis of strontium doped lanthanum manganite, the Second International Conference on the Characterization and Control of Interfaces for High Quality Advanced Materials, and Joining Technology for New Metallic Glasses and Inorganic Materials (ICCCI), Kurashiki, Japan, September 6-9, 2006.

3. **J. Chaichanawong**, K. Sato, H. Abe, K. Murata, T. Fukui, W. Tanthapanichakoon, T. Charinpanitkul, M. Naito, Microstructural control of LSM/YSZ composite cathode for lower temperature operation of SOFC, *accepted for* the Second International Conference on Nano/Micro Engineered Molecular System (IEEE-NEMS 2007), Bangkok, Thailand, January 16-19, 2007.

VITA

Mr. Jintawat Chaichanawong was born in Buriram, Thailand, on April 7, 1978. He entered King Mongkut's Institute of Technology Ladkrabang, Bangkok, in June, 1996. After earning the degree of Bachelor of Engineering in Chemical Engineering in March, 2000, he gained admission to the Graduate School of Chulalongkorn University in June 2000. In April 2003, he was awarded the degree of Master of Engineering in Chemical Engineering. After that, he continued to study in Ph.D. program under the Royal Golden Jubilee Scholarship, and he graduated in October 2006.